Research Paper

Analysis of immune-related signatures of lung adenocarcinoma identified two distinct subtypes: implications for immune checkpoint blockade therapy

Qinghua Wang[1], Meiling Li[1], Meng Yang[2], Yichen Yang[2], Fengju Song[1], Wei Zhang[3], Xiangchun Li[2], Kexin Chen[1]

[1]Department of Epidemiology and Biostatistics, National Clinical Research Center for Cancer, Key Laboratory of Molecular Cancer Epidemiology of Tianjin, Tianjin Medical University Cancer Institute and Hospital, Tianjin 300060, China
[2]Tianjin Cancer Institute, National Clinical Research Center for Cancer, Key Laboratory of Cancer Prevention and Therapy of Tianjin, Tianjin Medical University Cancer Institute and Hospital, Tianjin 300060, China
[3]Wake Forest Baptist Comprehensive Cancer Center, Wake Forest Baptist Medical Center, Winston-Salem, NC 27157, USA

Correspondence to: Kexin Chen, Xiangchun Li; **email:** chenkexin@tmu.edu.cn, lixiangchun@tmu.edu.cn
Keywords: lung adenocarcinoma, immune subtyping, immunotherapy, prognosis
Received: September 18, 2019 **Accepted:** January 27, 2020 **Published:** February 24, 2020

ABSTRACT

Immune checkpoint blockade (ICB) therapies have revolutionized the treatment of human cancers including lung adenocarcinoma (LUAD). However, our understanding of the immune subtyping of LUAD and its association with clinical response of immune checkpoint inhibitor remains incomplete. Here we performed molecular subtyping and association analysis of LUAD from the Cancer Genome Atlas (TCGA) and validated findings from TCGA cohort in 9 independent validation cohorts. We conducted consensus molecular subtyping with nonnegative matrix factorization (NMF). Potential response of ICB therapy was estimated with Tumor Immune Dysfunction and Exclusion (TIDE) algorithm. We identified 2 distinct subtypes of LUAD in TCGA cohort that were characterized by significantly different survival outcomes (i.e., high- and low-risk subtypes). The high-risk subtype was featured by lower TIDE score, upregulation of programmed death-ligand 1 (*PD-L1*) expression, and higher tumor mutation burden (TMB). The high-risk subtype also harbored significantly elevated cell cycle modulators CDK4/CDK6 and *TP53* mutation. These observations were validated in 9 independent LUAD cohorts. Our findings suggest that immune checkpoint blockade therapy may be efficacious for high-risk subtype of LUAD patients.

INTRODUCTION

Lung adenocarcinoma (LUAD) is a leading cause of cancer related death worldwide and accounts for about 40% of lung cancer patients [1]. Over the last decade, treatment regimens that target epidermal growth factor receptor and anaplastic lymphoma kinase have only benefitted a small fraction of LUAD patients [2, 3]. Clinically defined molecular subtyping of LUAD is in urgent need for precise treatment.

Programmed cell death protein 1/programmed cell death-ligand 1 (PD-1/PD-L1) axis is a critical immune checkpoint pathway that could downregulate response of immune system in lung cancer [4]. Enhanced PD-L1 expression level on tumor cells or tumor infiltrating lymphocytes leads to T cell exhaustion [5], therefore decreasing tumor-specific immune capacity and promoting tumor proliferation [6, 7]. Immune checkpoint blockade (ICB) therapy aimed at PD-1/PD-L1 could repress the negative regulatory signaling and unleash T

cell from exhausted status [7]. ICB therapy can reverse the immunosuppressive microenvironment by decreasing the potential of tumor immune escape, therefore, resulting in noteworthy improvement of prognosis [8, 9]. High expression level of PD-L1 was approved by The Food and Drug Administration (FDA) as a biomarker to receive pembrolizumab therapy in non-small-cell lung cancer (NSCLC) [8].

Tumor mutation burden (TMB) is an indicator implicated in better response to ICB treatment, which is independent of PD-L1 expression level [10, 11]. An integrated analysis of 27 cancer types reported positive association between TMB and benefit of ICB treatment [12]. In present clinical practice, the proportion of patients benefitted from ICB therapy remains low. Therefore, the development of new biomarkers to select patient for ICB response rate is definitely required [13, 14].

Tumor Immune Dysfunction and Exclusion (TIDE) algorithm is a computational method using gene expression profile to predict the ICB response in NSCLC and melanoma [15]. TIDE uses a set of gene expression markers to estimate 2 distinct mechanisms of tumor immune evasion, including dysfunction of tumor infiltration cytotoxic T lymphocytes (CTL) and exclusion of CTL by immunosuppressive factors. Patients with higher TIDE score have a higher chance of antitumor immune escape, thus exhibiting lower response rate of ICB treatment [15]. The TIDE score was shown to have a higher accuracy than PD-L1 expression level and TMB in predicting survival outcome of cancer patients treated with ICB agents [15–18]. Several recent studies have reported its utility in predicting or evaluating the ICB therapy efficacy [18–22].

In this study, we performed consensus clustering analysis for LUAD based on immune gene expression signatures and identified 2 subtypes. These 2 subtypes were characterized by significantly different survival outcomes (i.e., low- versus high-risk subtypes), TIDE scores, PD-L1 expression, TMB and enrichment of cell cycle signaling. The high-risk subtype is presumably efficacious towards ICB treatment.

RESULTS

Identification of LUAD subtypes with prognostic significance

A list of 2,995 immune-related genes (See Materials and Methods) was compiled, 433 of which were significantly associated with overall survival (all FDR < 0.05; Supplementary Table 1) in the TCGA LUAD cohort (n = 502). Using this 433-gene panel, we identified 2 distinct LUAD subtypes (Figure 1A and Supplementary Figure 1) by performing consensus clustering analysis. These 2 subtypes were significantly different in survival (HR: 1.99, 95% CI: 1.43-2.76, Log rank P < 0.001; Figure 1B) and we referred them as high-risk and low-risk subtypes. After adjusting for age, gender, stage and smoking status, this association remained statistically significant (HR: 1.80, 95% CI: 1.28-2.53, P < 0.001; Figure 1C).

To verify the findings in TCGA LUAD cohort, we applied consensus clustering analysis using the aforementioned 433 immune-related genes and performed survival analysis in 9 additional independent LUAD cohorts. Our analysis showed that these 2 distinct subtypes identified in TCGA LUAD cohort were also identified in these 9 validation datasets, in that high-risk group was associated with worse survival outcome (HR range: 1.69 [95% CI: 1.29-2.21, Log rank P < 0.001] to 4.29 [95% CI: 2.14-8.65, Log rank P < 0.001]; Figure 2A–2I). These associations remained statistically significant after controlling for other confounding factors (Supplementary Figure 2A–2I). Result of another LUAD dataset GSE81089 (n = 108) showed a consistent trend although did not reach statistical significance (HR: 1.59, 95% CI: 0.89-2.85, Log rank P = 0.11; Supplementary Figure 3A). No significant association was observed for lung squamous cell carcinoma from TCGA dataset (HR: 1.03, 95% CI: 0.78-1.35, Log rank P = 0.86; Supplementary Figure 3B).

We obtained an accuracy of 0.947 with 126 genes (Supplementary Figure 4A and Supplementary Table 2) by applying recursive feature elimination to reduce the number of genes. The prognostic significance of high-risk versus low-risk subtypes was maintained using these 126 genes in TCGA and 9 validation cohorts (HR range: 1.84 [95% CI: 1.37-2.48, Log rank P < 0.001] to 5.99 [95% CI: 2.72-12.23, Log rank P < 0.001]; Supplementary Figure 4B–4K).

Predictive ICB response of identified LUAD subtypes

In the TCGA LUAD cohort, the TIDE score was significantly lower in high-risk subtype compared with low-risk subtype (Wilcoxon rank-sum test, P < 0.001; Figure 3A). The difference remained statistically significant after adjusting for age, gender, stage and smoking status (OR: 0.13, 95% CI: 0.08-0.20, P < 0.001; Figure 3B). This association was verified in 9 independent cohorts using univariate analysis (Wilcoxon rank-sum test, P < 0.05; Figure 3C), and 8 of these 9 cohorts showed the same association through multivariate logistic model (P < 0.001; Supplementary Figure 5A–5I). These discoveries suggested that patients of high-risk subtype may be more sensitive to ICB therapy as judged by the TIDE score.

Differences of *PD-L1* expression and TMB between 2 LUAD subtypes

The expression of *PD-L1* was significantly higher in high-risk group versus low-risk group in TCGA (Wilcoxon rank-sum test, $P = 0.003$; Figure 4A). Consistent association was also observed in 7 of 9 validation cohorts (Wilcoxon rank-sum test, $P < 0.05$; Figure 4B). We could not validate this association in the other 2 cohorts (GSE68465 and GSE11969) due to the lack of *PD-L1* probes on the expression chip used.

Patients in high-risk subtype had a significantly higher mutation load in TCGA LUAD samples (Wilcoxon rank-sum test, $P < 0.001$; Figure 4C). Associations between high-risk subtype and TMB remained statistically significant (OR: 3.99, 95% CI: 2.19-7.46, $P < 0.001$; Figure 4D) after taking into account mutational signatures implicated in age-related deamination of 5-methylcytosine (signature 1), overactivity of mRNA-editing enzyme APOBEC (signature 2) and tobacco smoking-related C>A mutations (signature 4) (Supplementary Figure 6), and mutations in genes related to DNA damage repair (DDR) such as *POLE*, *BRCA1/2*, and *TP53*. Additionally, we found that high-risk subtype harbored a significantly higher nonsynonymous mutation load (Wilcoxon rank-sum test, $P < 0.001$; Figure 4E).

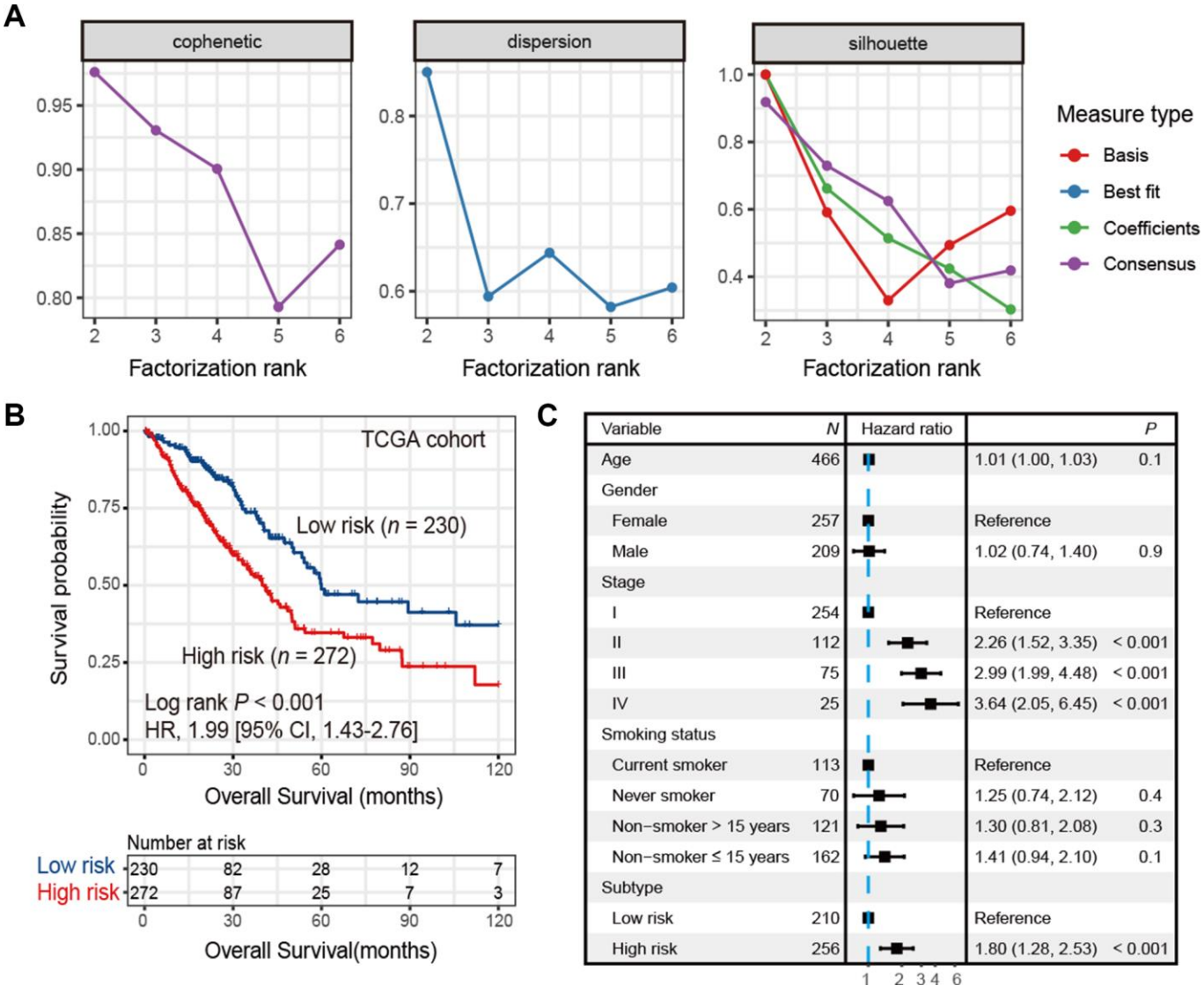

Figure 1. Identification of high-risk and low-risk subtypes of LUAD in TCGA cohort by consensus clustering. (**A**) The relationship between cophenetic, dispersion and silhouette coefficients with respect to number of clusters. (**B**) Kaplan-Meier survival plot of the high-risk versus the low-risk subtype. (**C**) Forest plot representation of multivariate Cox model depicted association between overall survival and LUAD subtypes with other clinical factors taken into account.

In TCGA LUAD cohort, association of TMB with survival was not significant. Associations of TIDE score and *PD-L1* expression with survival were not significant across TCGA LUAD cohort and the 9 validation cohorts (Supplementary Figure 7).

Functional characterization of the high-risk subtype

Cell cycle relevant signaling pathways were frequently activated in high-risk group as compared with low-risk group (FDR < 0.001; Figure 5A). Molecular markers involved in cell cycle checkpoint were significantly upregulated in the high-risk subtype (Wilcoxon rank-sum test, $P < 0.001$; Figure 5B). The cell cycle checkpoint markers analyzed include *CCND1*, *CCNE1*, *CDK2*, *CDK4* and *CDK6* in G1/S checkpoint, and *CCNA2* and *CDK1* in G2/M checkpoint. Previous studies reported that CDK4 and CDK6 inhibitors could enhance T cell activity [23] and reverse the T cell exclusion signature [24] to obtain better ICB treatment response.

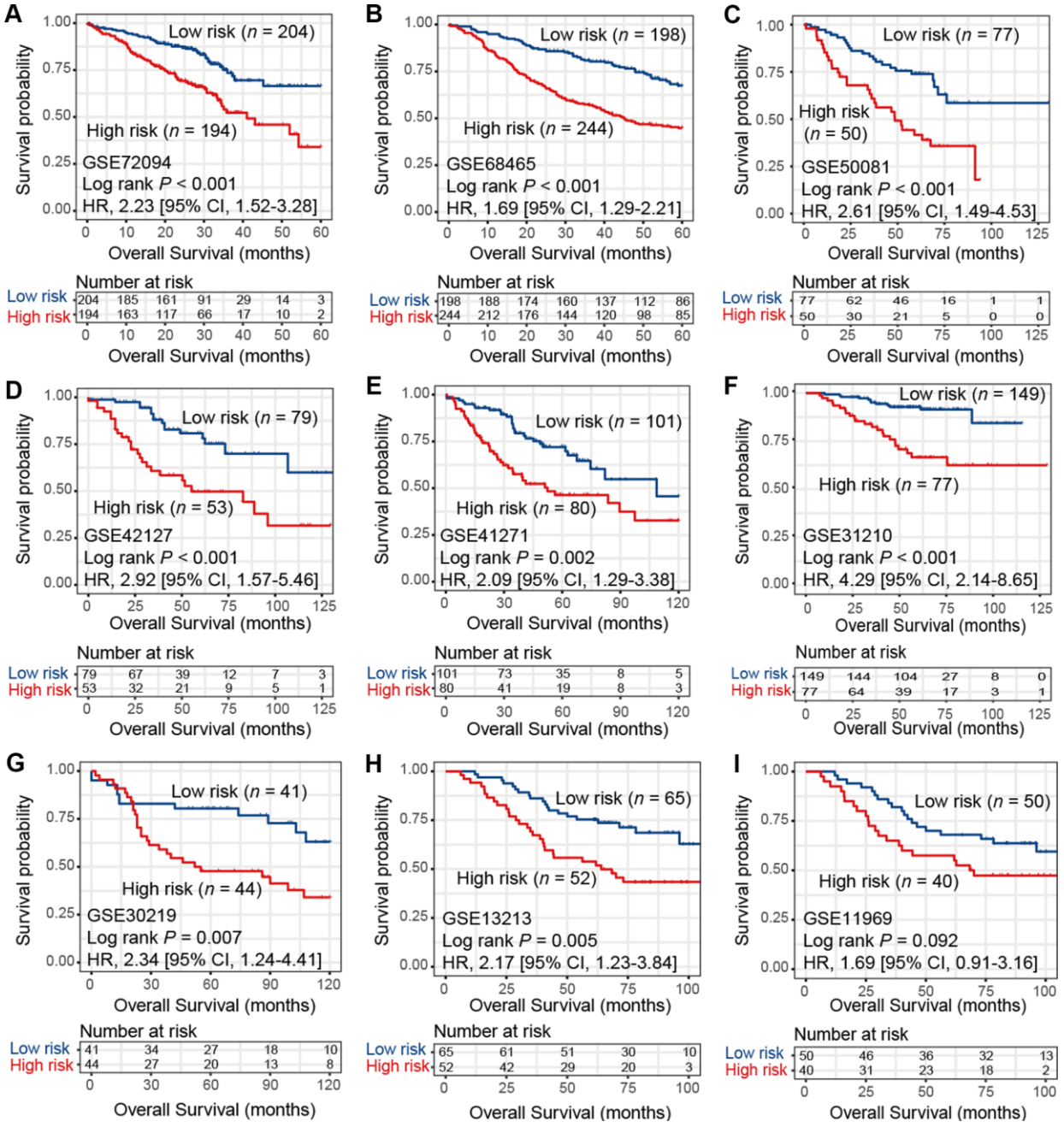

Figure 2. Kaplan-Meier plots of high-risk and low-risk subtypes of LUAD in 9 validation cohorts of (**A**) GSE72094, (**B**) GSE68465, (**C**) GSE50081, (**D**) GSE42127, (**E**) GSE41271, (**F**) GSE31210, (**G**) GSE30219, (**H**) GSE13213, and (**I**) GSE11969.

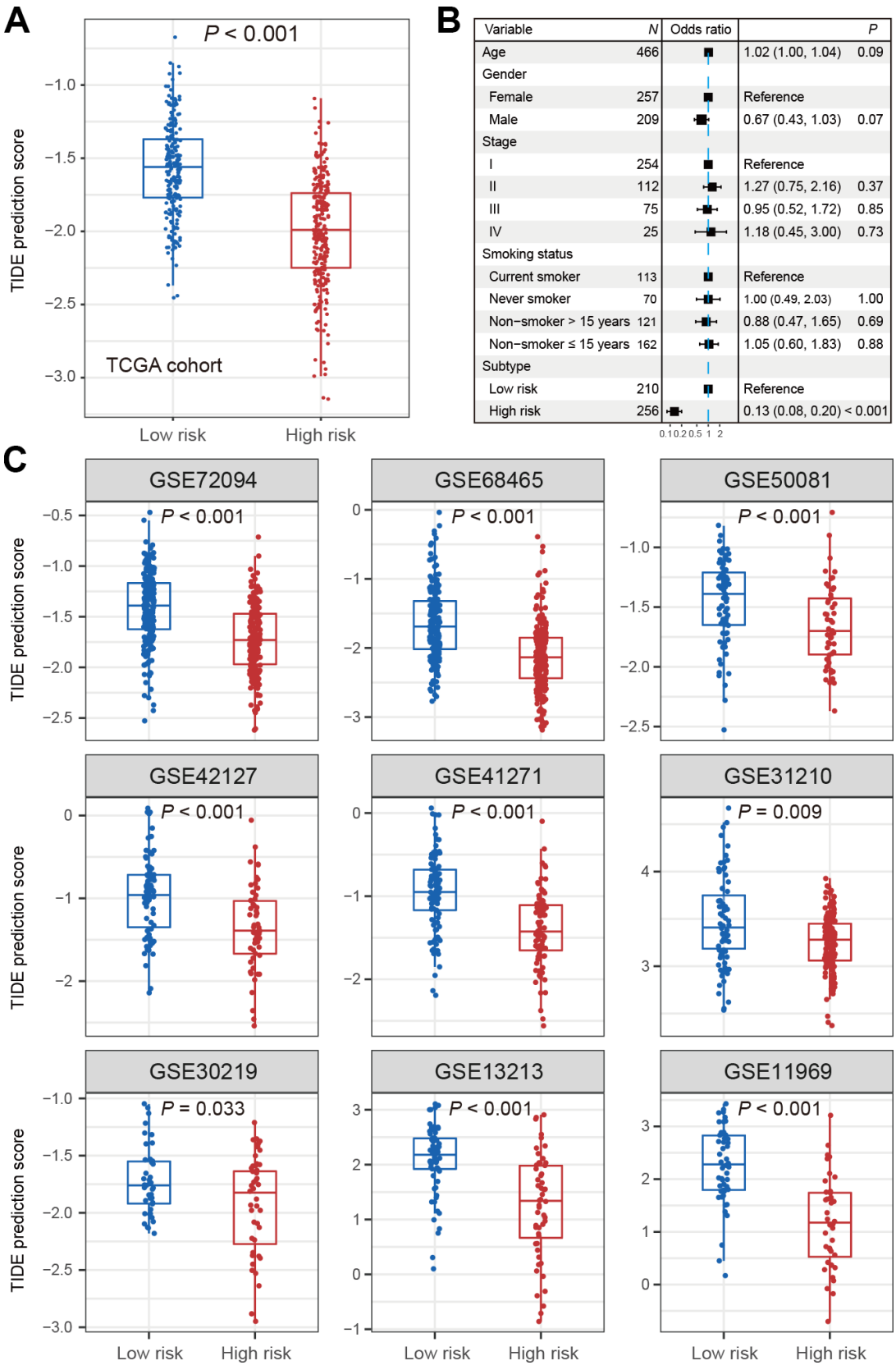

Figure 3. Distribution of TIDE scores in high-risk subtype of LUAD versus low-risk subtype of LUAD. (**A**) Boxplot representation of TIDE scores in the high-risk group versus low-risk group in TCGA LUAD cohort. (**B**) Forest plot representation of multivariate model with adjustment for confounding factors in TCGA cohort. (**C**) Distribution of TIDE scores in 9 independent validation cohorts.

Mutation patterns of SMGs in relation to LUAD subtypes

We identified 23 significantly mutated genes (SMGs) in TCGA LUAD cohort (Supplementary Figure 8). *TP53*, *NAV3*, *COL11A1*, *KEAP1* and *SMARCA4* were more frequently mutated in high-risk subtype (Fisher exact test, OR > 1, $P < 0.05$; Figure 6). Association of these SMGs with high-risk subtype remained significant after including age, gender, stage and smoking status (OR > 1, $P < 0.01$; Supplementary Figure 9). Higher mutation frequency of *TP53* in high-risk subtype was observed in 3 validation cohorts that had *TP53* mutation data (OR > 1, $P < 0.01$; Supplementary Figure 10). Mutation data of *NAV3*, *COL11A1*, *KEAP1* and *SMARCA4* of the aforementioned 3 validation cohorts was unavailable. In addition, we found that patients in high-risk subtype were more likely to be male, current smoker, and at advanced clinical stage (chi-square test, $P < 0.001$; Supplementary Table 3).

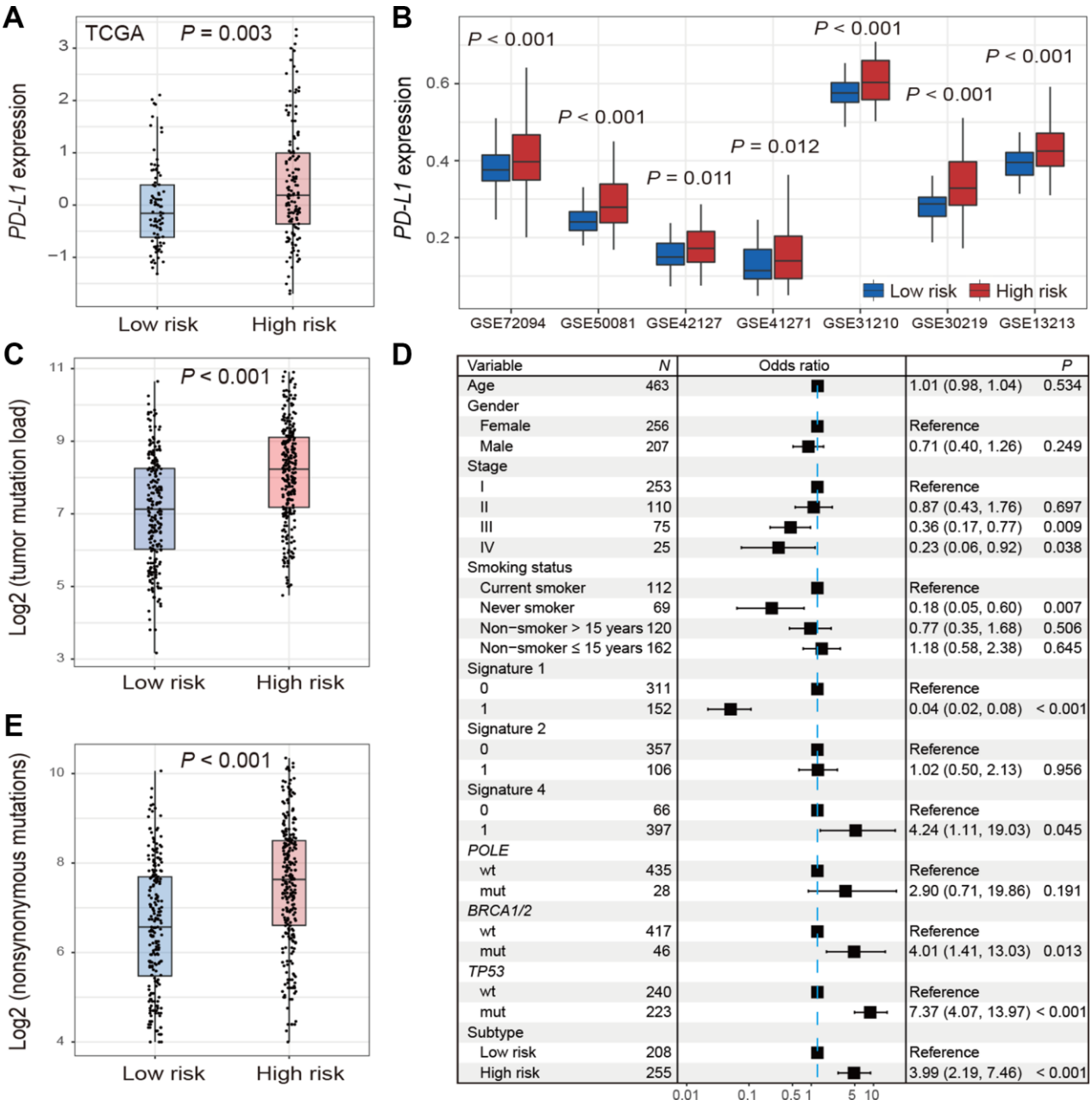

Variable	N	Odds ratio	P
Age	463	1.01 (0.98, 1.04)	0.534
Gender			
Female	256	Reference	
Male	207	0.71 (0.40, 1.26)	0.249
Stage			
I	253	Reference	
II	110	0.87 (0.43, 1.76)	0.697
III	75	0.36 (0.17, 0.77)	0.009
IV	25	0.23 (0.06, 0.92)	0.038
Smoking status			
Current smoker	112	Reference	
Never smoker	69	0.18 (0.05, 0.60)	0.007
Non−smoker > 15 years	120	0.77 (0.35, 1.68)	0.506
Non−smoker ≤ 15 years	162	1.18 (0.58, 2.38)	0.645
Signature 1			
0	311	Reference	
1	152	0.04 (0.02, 0.08)	< 0.001
Signature 2			
0	357	Reference	
1	106	1.02 (0.50, 2.13)	0.956
Signature 4			
0	66	Reference	
1	397	4.24 (1.11, 19.03)	0.045
POLE			
wt	435	Reference	
mut	28	2.90 (0.71, 19.86)	0.191
BRCA1/2			
wt	417	Reference	
mut	46	4.01 (1.41, 13.03)	0.013
TP53			
wt	240	Reference	
mut	223	7.37 (4.07, 13.97)	< 0.001
Subtype			
Low risk	208	Reference	
High risk	255	3.99 (2.19, 7.46)	< 0.001

Figure 4. Distribution of *PD-L1* expression and tumor mutation burden and their associations with the high-/low-risk subtypes of LUAD. (**A**, **B**) Difference in the *PD-L1* expression in TCGA and validation cohorts stratified by high-/low-risk subtypes of LUAD. (**C**–**E**) Distribution and association of mutation burden in the high-risk group versus low-risk group.

DISCUSSION

We uncovered 2 prognostic subtypes of LUAD by analyzing 2,300 LUAD samples from TCGA LUAD cohort and 9 independent validation cohorts. The high-risk subtype has significantly lower TIDE score, higher *PD-L1* expression and higher TMB. Pathway analysis suggested that high-risk group was featured by activated cell cycle signaling. *TP53* mutation was more frequently mutated in the high-risk subtype.

We observed that TIDE score was significantly lower in high-risk subtype than low-risk subtype via univariate regression analysis in TCGA LUAD cohort and 9 validation cohorts. The difference remained statistically significant in multivariate analysis among these cohorts except GSE30219, this is probably due to smaller sample size of GSE30219 cohort (n = 85) as compared with the other LUAD cohorts. These findings suggested that patients of high-risk subtype may be more sensitive to ICB treatment

Based on the KEYNOTE-001 clinical trial, PD-L1 high expression was an essential condition for the use of pembrolizumab in NSCLC [8, 25]. Several studies have reported that PD-L1 high expression was correlated to elevated response rate and survival benefit in ICB therapy of NSCLC, chronic lymphocytic leukemia and urothelial cancer [26–28]. However, in the clinical trial CHECKMATE-032 that enrolled patients with urothelial cancer, no significant difference was observed in response rate between PD-L1 positive and negative subgroups [29]. This suggests that our understanding of association between PD-L1 and ICB

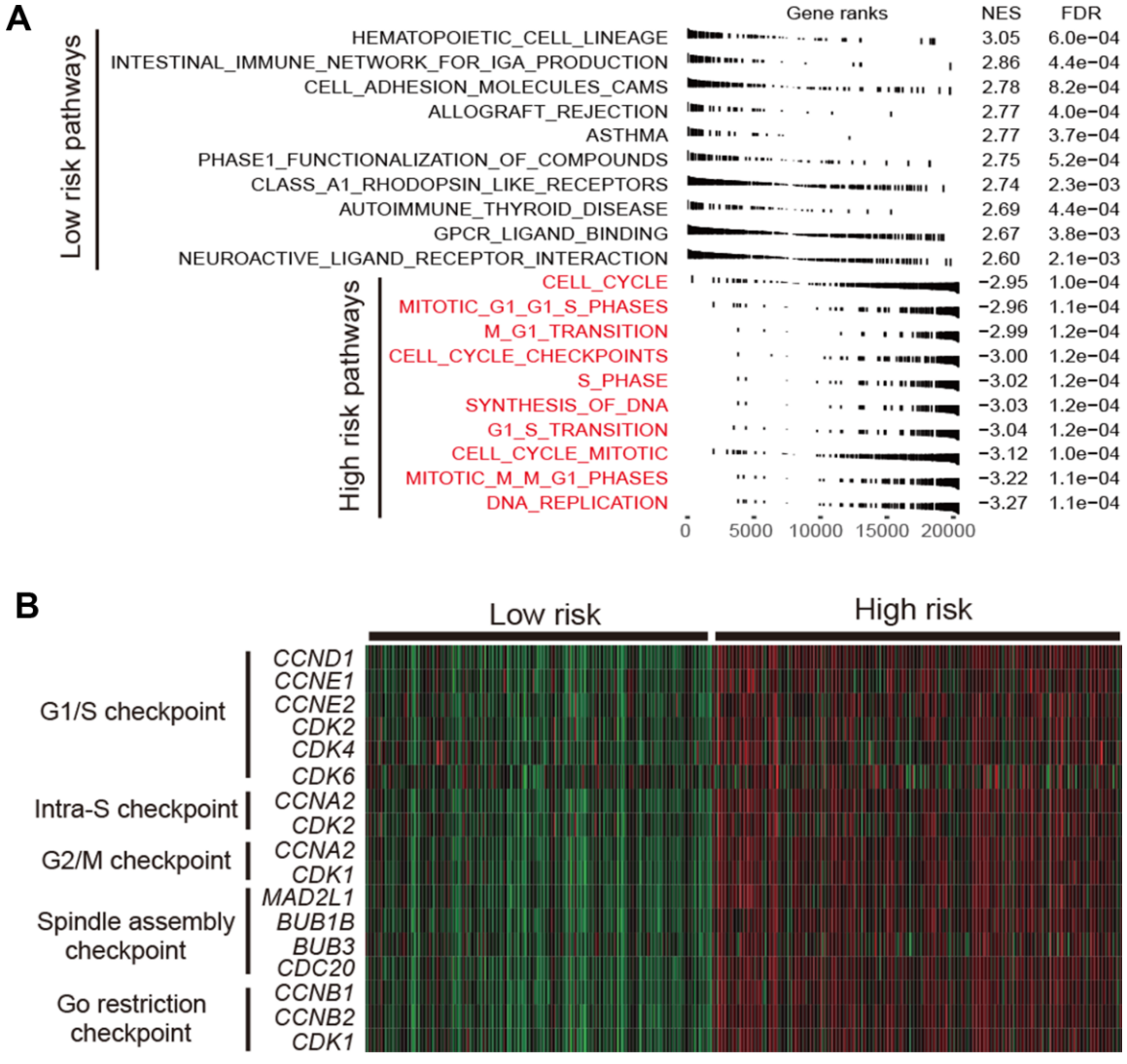

Figure 5. Functional annotation in high-/low-risk subtypes of LUAD. (**A**) Dysregulation of signaling pathways stratified by identified LUAD subtypes. (**B**) Expression profiles of cell cycle checkpoint markers in the high-risk group versus low-risk group.

response is far from complete and that new markers associated with ICB response are needed. A possible explanation for this inconsistency is attributed to different criterion used for evaluating high and low PD-L1 expression [30]. TMB is emerging as a potential biomarker for predicting response of ICB therapy. Three clinical trials including KEYNOTE-001, CHECKMATE-026 and CHECKMATE-227 showed that patients had high TMB could benefit more from ICB therapy in NSCLC [31–33]. In our study, the high-risk subtype had significantly higher *PD-L1* expression and TMB, suggesting a greater potential of ICB therapy response.

Consistent with our findings, Seo et al. identified the immune-defective and immune-competent subtypes in LUAD, and the immune-competent subtype was characterized by activated microenvironment and elevated expression of immune checkpoint genes [34]. In our study, we observed a significant prognostic difference between the high-risk and low-risk subtypes. However, a survival difference was not observed for the 2 subtypes proposed by Seo et al. A recent study from Song et al. also reported identification of the high-risk and low-risk subtypes of LUAD [35]. The high-risk subtype in this study exhibited worse survival outcome and a higher tumor mutation load, which supports our result that the high-risk subtype may be more responsive to immune checkpoint therapy because of the higher tumor mutation load. The prognostic significance of high-risk and low-risk subtypes from our study was validated in GSE31210, a validation dataset used in Song et al. research, whereas subtypes proposed by Song et al. was not significant. Taken together, the gene panels used in our study for molecular subtyping are more generalizable and robust given that we included more validation sets (n=9) as compared with 4 validation cohorts used by Song et al.

Cell cycle relevant pathways and checkpoint markers contributed mostly to the worse prognosis of high-risk subtype were significantly upregulated. These observations suggested the high-risk patients may be suitable to receive cell cycle inhibitors. Previous studies

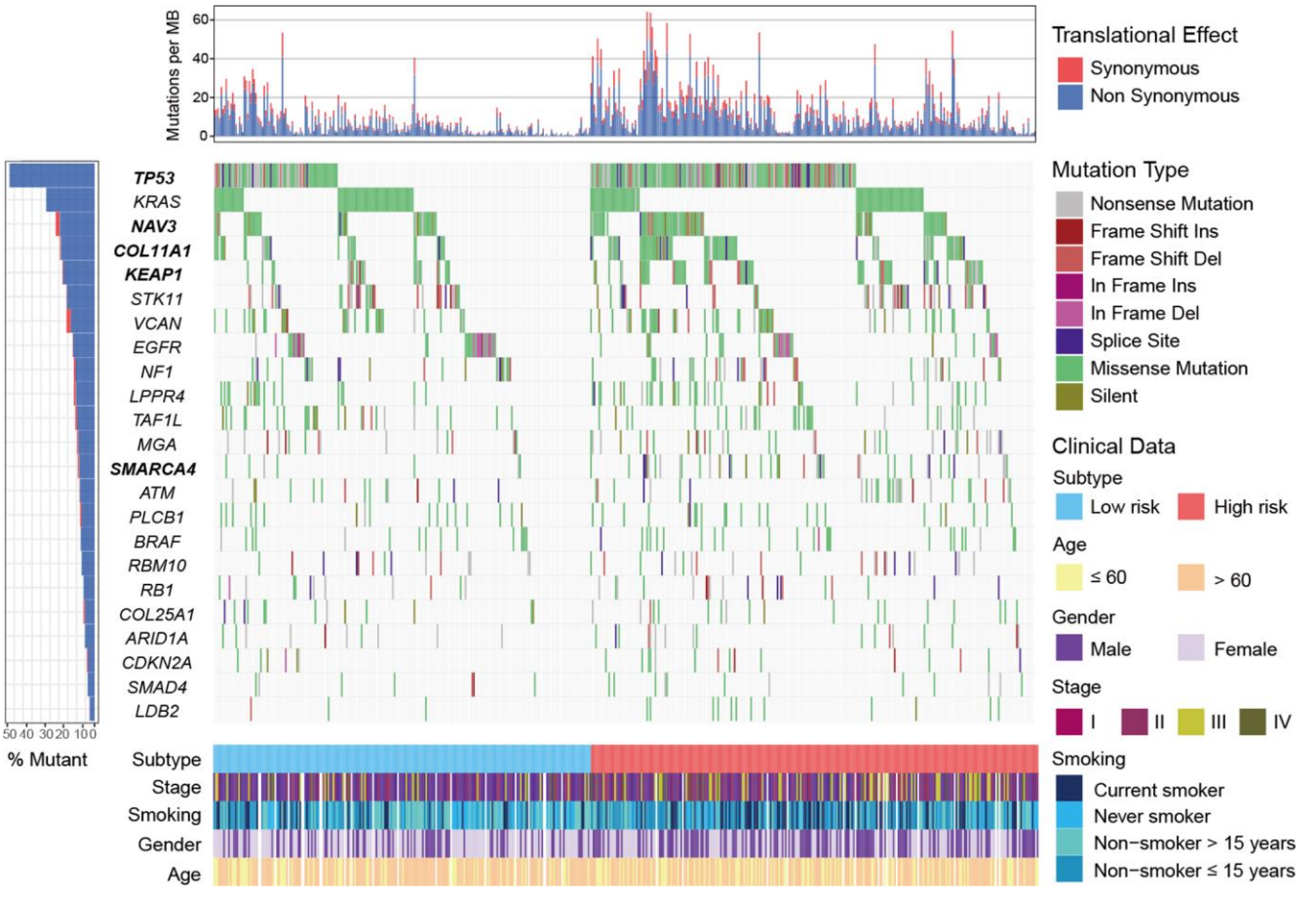

Figure 6. Mutational landscape of SMGs in TCGA LUAD cohort stratified by high-/low-risk subtypes. SMGs with significantly different mutation rate were highlighted in bold.

showed that CDK4 and CDK6 inhibitors enhanced the response of ICB in mouse models due to their ability to elevate expression of endogenous retroviruses [36] that was associated with T cell activity [23] and ICB response [37]. Another study reported that the T cell exclusion signature was predictive of poor ICB response, however, CDK4 and CDK6 inhibitors could reverse this signature to get a better response in *in vitro* experiments in melanoma [24]. The combination therapy of cell cycle inhibitors and ICB agents may be more effective for the high-risk patients.

TP53 was frequently mutated in the high-risk subtype and its mutation was reported to be associated with poorer prognosis [38, 39]. Patients harbored mutations of *TP53* had a higher TMB owing to loss of DNA repair function (Figure 4D). Recent study reported that *TP53* mutations significantly induced the expression of immune checkpoints and activated T-effector and interferon-γ signature in LUAD, suggesting *TP53* mutation patients would be more responsive to checkpoint blockade [40]. Patients of high-risk subtype were more likely to be current smokers. Higher response rate of ICB treatment was observed in smokers of NSCLC [41], typically due to high mutation burden generated by the mutagenic effects of cigarette smoke [42]. These 2 factors may underlie the response to ICB therapy for patients of high-risk group.

There are several limitations in this study. Firstly, gene expression data used in our study was from different platforms, this difference may introduce bias in the analysis procedure. Secondly, results derived from TCGA LUAD mutational landscape were not validated in independent datasets due to the unavailability of mutation data in validation sets. Thirdly, we lacked an in-house validation set.

In summary, we identified 2 prognostically and clinically relevant subtypes of LUAD. Molecular markers suggest that patients from the high-risk subtype may be more responsive to ICB therapy, which needs to be tested in future clinical trials.

MATERIALS AND METHODS

Collection of genomic data

We collected gene expression profiles of 502 LUAD samples from TCGA-LUAD cohort (https://gdc.cancer.gov) and 1,798 samples from 9 cohorts in Gene Expression Omnibus (GEO) repository (https://www.ncbi.nlm.nih.gov/geo/) (Supplementary Table 4). In total, we obtained 2,300 LUAD samples from 10 independent cohorts (Supplementary Table 5). We also collected clinical data for each cohort. All gene expression data were uniformly normalized. For genes with multiple probes, their expression levels were calculated as the mean expression level of these probes. Only TCGA cohort contained genomic mutation data used in our study. A flow chart to depict the study design was shown in Supplementary Figure 11.

Identification of immune-related genes associated with prognosis

We obtained 2,995 immune-related genes from 160 immune signatures curated in the TCGA pan-cancer immune landscape project [43], which was based on 11 immune relevant studies [44–54] (Supplementary Materials and Methods). We used univariate Cox proportional hazards model to examine the associations between gene expression and overall survival. Genes with false discovery rate (FDR) less than 0.05 were considered to be statistically significant and included in consensus clustering analysis. Further feature selection was conducted by using recursive feature elimination (RFE) with random forest as classifier and 10-fold cross-validation method in *R* package *caret* (version 6.0-82).

Consensus molecular subtyping with NMF

We used nonnegative matrix factorization (NMF) to perform molecular subtyping [55, 56]. Specifically, NMF was applied to gene expression matrix A that contained prognostically significant immune-related genes aforementioned. Matrix A was factorized into 2 nonnegative matrices W and H (i.e., $A \approx WH$). Repeated factorization of matrix A was performed and its outputs were aggregated to obtain consensus clustering of LUAD samples. The optimal number of subtypes was selected according to cophenetic, dispersion, and silhouette coefficients [57]. The consensus clustering was conducted with *R* package *NMF* (version 0.21.0) [58]. The NMF method was also used to extract mutational signatures based on the framework proposed by a previously study [59]. The *R* code was available in Supplementary Materials and Methods.

Prediction of ICB therapy response

Potential ICB response was predicted with TIDE algorithm [15].

Gene set enrichment analysis

The *R* package *limma* (version 3.38.3) [60] and *DESeq2* (version 1.22.2) [61] were used to calculate the differential expressed t statistics for microarray and RNA sequencing data. We used t statistic as input to *R* function *fgsea* that implemented in *fgsea* package

(version 1.6.0) to perform gene set enrichment analysis (GSEA). Signaling pathways in Molecular Signatures Database (MSigDB) were used in GSEA [62].

Identification of significantly mutated genes

Significantly mutated genes (SMGs) were identified using MutSigCV algorithm [63]. The significant enrichment of non-silent somatic mutations of a gene was measured by MutSigCV through addressing mutational context specific background mutation rates. A gene was considered an SMG if it meets these criteria: statistically significant ($q < 0.1$), expressed in TCGA LUAD data [64] and encyclopedia of cell lines [65], and mutation rate greater than 3%.

Statistical analyses

R software 3.5.1 was applied in this study for the statistical analyses. Univariate and multivariate Cox proportional hazards model were used to analyze the association between subtypes and prognosis with *R survival* package. Survival curve was drawn with Kaplan-Meier method and Log-rank test was used to evaluate difference between survival curves. Association between mutation rate of SMGs and 2 subtypes was evaluated by Fisher's exact test. Multivariate logistic regression was performed to test the association between SMGs and identified LUAD subtypes by taking into account confounding factors. The continuous and categorical variables between 2 subtypes were compared using two-sided Wilcoxon rank-sum test and chi-square test, respectively. Benjamini-Hochberg method was used to adjust for multiple hypothesis testing [61].

Abbreviations

CTL: cytotoxic T lymphocytes; DDR: DNA damage repair; FDA: Food and Drug Administration; FDR: false discovery rate; GEO: Gene Expression Omnibus; GSEA: gene set enrichment analysis; LUAD: lung adenocarcinoma; MSigDB: Molecular Signatures Database; NMF: nonnegative matrix factorization; NSCLC: non-small-cell lung cancer; *PD-L1*: programmed death-ligand 1; RFE: recursive feature elimination; SMGs: significantly mutated genes; TCGA: The Cancer Genome Atlas; TIDE: Tumor Immune Dysfunction and Exclusion; TMB: tumor mutation burden.

AUTHOR CONTRIBUTIONS

KXC and XCL designed this study; KXC, XCL, and QHW developed the methodology and acquired the related data; XCL, QHW, MLL, MY, YCY, and FJS performed data analysis and interpretation; XCL, KXC, WZ and QHW drafted and revised the manuscript; KXC and XCL supervised this study.

ACKNOWLEDGMENTS

We would like to thank Prof. Wei Zhang at the Wake Forest Baptist Comprehensive Cancer Center for his valued suggestions and editing of this manuscript.

CONFLICTS OF INTEREST

All authors declare no conflicts of interest.

FUNDING

The study has been supported by the Program for Changjiang Scholars and Innovative Research Team in University in China (IRT_14R40) and National Natural Science Foundation of China (NSFC) (no. 31801117).

REFERENCES

1. Shi J, Hua X, Zhu B, Ravichandran S, Wang M, Nguyen C, Brodie SA, Palleschi A, Alloisio M, Pariscenti G, Jones K, Zhou W, Bouk AJ, et al. Somatic Genomics and Clinical Features of Lung Adenocarcinoma: A Retrospective Study. PLoS Med. 2016; 13:e1002162. https://doi.org/10.1371/journal.pmed.1002162 PMID:27923066

2. Vargas AJ, Harris CC. Biomarker development in the precision medicine era: lung cancer as a case study. Nat Rev Cancer. 2016; 16:525–37. https://doi.org/10.1038/nrc.2016.56 PMID:27388699

3. Seo JS, Ju YS, Lee WC, Shin JY, Lee JK, Bleazard T, Lee J, Jung YJ, Kim JO, Shin JY, Yu SB, Kim J, Lee ER, et al. The transcriptional landscape and mutational profile of lung adenocarcinoma. Genome Res. 2012; 22:2109–19. https://doi.org/10.1101/gr.145144.112 PMID:22975805

4. Kythreotou A, Siddique A, Mauri FA, Bower M, Pinato DJ. Pd-L1. J Clin Pathol. 2018; 71:189–94. https://doi.org/10.1136/jclinpath-2017-204853 PMID:29097600

5. Witt DA, Donson AM, Amani V, Moreira DC, Sanford B, Hoffman LM, Handler MH, Levy JM, Jones KL, Nellan A, Foreman NK, Griesinger AM. Specific expression of PD-L1 in RELA-fusion supratentorial ependymoma: implications for PD-1-targeted therapy. Pediatr Blood Cancer. 2018; 65:e26960. https://doi.org/10.1002/pbc.26960 PMID:29350470

6. Zheng B, Ren T, Huang Y, Sun K, Wang S, Bao X, Liu K, Guo W. PD-1 axis expression in musculoskeletal tumors and antitumor effect of nivolumab in osteosarcoma model of humanized mouse. J Hematol Oncol. 2018; 11:16. https://doi.org/10.1186/s13045-018-0560-1 PMID:29409495

7. Xu-Monette ZY, Zhang M, Li J, Young KH. PD-1/PD-L1 Blockade: Have We Found the Key to Unleash the Antitumor Immune Response? Front Immunol. 2017; 8:1597. https://doi.org/10.3389/fimmu.2017.01597 PMID:29255458

8. Garon EB, Rizvi NA, Hui R, Leighl N, Balmanoukian AS, Eder JP, Patnaik A, Aggarwal C, Gubens M, Horn L, Carcereny E, Ahn MJ, Felip E, et al, and KEYNOTE-001 Investigators. Pembrolizumab for the treatment of non-small-cell lung cancer. N Engl J Med. 2015; 372:2018–28. https://doi.org/10.1056/NEJMoa1501824 PMID:25891174

9. Brahmer J, Reckamp KL, Baas P, Crinò L, Eberhardt WE, Poddubskaya E, Antonia S, Pluzanski A, Vokes EE, Holgado E, Waterhouse D, Ready N, Gainor J, et al. Nivolumab versus Docetaxel in Advanced Squamous-Cell Non-Small-Cell Lung Cancer. N Engl J Med. 2015; 373:123–35. https://doi.org/10.1056/NEJMoa1504627 PMID:26028407

10. Hodges TR, Ott M, Xiu J, Gatalica Z, Swensen J, Zhou S, Huse JT, de Groot J, Li S, Overwijk WW, Spetzler D, Heimberger AB. Mutational burden, immune checkpoint expression, and mismatch repair in glioma: implications for immune checkpoint immunotherapy. Neuro Oncol. 2017; 19:1047–57. https://doi.org/10.1093/neuonc/nox026 PMID:28371827

11. Rizvi H, Sanchez-Vega F, La K, Chatila W, Jonsson P, Halpenny D, Plodkowski A, Long N, Sauter JL, Rekhtman N, Hollmann T, Schalper KA, Gainor JF, et al. Molecular Determinants of Response to Anti-Programmed Cell Death (PD)-1 and Anti-Programmed Death-Ligand 1 (PD-L1) Blockade in Patients With Non-Small-Cell Lung Cancer Profiled With Targeted Next-Generation Sequencing. J Clin Oncol. 2018; 36:633–41. https://doi.org/10.1200/JCO.2017.75.3384 PMID:29337640

12. Yarchoan M, Hopkins A, Jaffee EM. Tumor Mutational Burden and Response Rate to PD-1 Inhibition. N Engl J Med. 2017; 377:2500–01. https://doi.org/10.1056/NEJMc1713444 PMID:29262275

13. Ancevski Hunter K, Socinski MA, Villaruz LC. PD-L1 Testing in Guiding Patient Selection for PD-1/PD-L1 Inhibitor Therapy in Lung Cancer. Mol Diagn Ther. 2018; 22:1–10. https://doi.org/10.1007/s40291-017-0308-6 PMID:29119407

14. Janjigian YY, Sanchez-Vega F, Jonsson P, Chatila WK, Hechtman JF, Ku GY, Riches JC, Tuvy Y, Kundra R, Bouvier N, Vakiani E, Gao J, Heins ZJ, et al. Genetic Predictors of Response to Systemic Therapy in Esophagogastric Cancer. Cancer Discov. 2018; 8:49–58. https://doi.org/10.1158/2159-8290.CD-17-0787 PMID:29122777

15. Jiang P, Gu S, Pan D, Fu J, Sahu A, Hu X, Li Z, Traugh N, Bu X, Li B, Liu J, Freeman GJ, Brown MA, et al. Signatures of T cell dysfunction and exclusion predict cancer immunotherapy response. Nat Med. 2018; 24:1550–58. https://doi.org/10.1038/s41591-018-0136-1 PMID:30127393

16. Kaderbhaï C, Tharin Z, Ghiringhelli F. The Role of Molecular Profiling to Predict the Response to Immune Checkpoint Inhibitors in Lung Cancer. Cancers (Basel). 2019; 11:11. https://doi.org/10.3390/cancers11020201 PMID:30744168

17. Keenan TE, Burke KP, Van Allen EM. Genomic correlates of response to immune checkpoint blockade. Nat Med. 2019; 25:389–402. https://doi.org/10.1038/s41591-019-0382-x PMID:30842677

18. Wang S, He Z, Wang X, Li H, Liu XS. Antigen presentation and tumor immunogenicity in cancer immunotherapy response prediction. eLife. 2019; 8:8. https://doi.org/10.7554/eLife.49020 PMID:31767055

19. Liu D, Schilling B, Liu D, Sucker A, Livingstone E, Jerby-Amon L, Zimmer L, Gutzmer R, Satzger I, Loquai C, Grabbe S, Vokes N, Margolis CA, et al. Integrative molecular and clinical modeling of clinical outcomes to PD1 blockade in patients with metastatic melanoma. Nat Med. 2019; 25:1916–27. https://doi.org/10.1038/s41591-019-0654-5 PMID:31792460

20. Bretz AC, Parnitzke U, Kronthaler K, Dreker T, Bartz R, Hermann F, Ammendola A, Wulff T, Hamm S. Domatinostat favors the immunotherapy response by modulating the tumor immune microenvironment (TIME). J Immunother Cancer. 2019; 7:294. https://doi.org/10.1186/s40425-019-0745-3 PMID:31703604

21. Pallocca M, Angeli D, Palombo F, Sperati F, Milella M, Goeman F, De Nicola F, Fanciulli M, Nisticò P, Quintarelli C, Ciliberto G. Combinations of immuno-checkpoint inhibitors predictive biomarkers only marginally improve their individual accuracy. J Transl Med. 2019; 17:131. https://doi.org/10.1186/s12967-019-1865-8 PMID:31014354

22. George AP, Kuzel TM, Zhang Y, Zhang B. The Discovery of Biomarkers in Cancer Immunotherapy. Comput Struct Biotechnol J. 2019; 17:484–97. https://doi.org/10.1016/j.csbj.2019.03.015 PMID:31011407

23. Rooney MS, Shukla SA, Wu CJ, Getz G, Hacohen N. Molecular and genetic properties of tumors associated with local immune cytolytic activity. Cell. 2015; 160:48–61. https://doi.org/10.1016/j.cell.2014.12.033 PMID:25594174

24. Jerby-Arnon L, Shah P, Cuoco MS, Rodman C, Su MJ, Melms JC, Leeson R, Kanodia A, Mei S, Lin JR, Wang S, Rabasha B, Liu D, et al. A Cancer Cell Program Promotes T Cell Exclusion and Resistance to Checkpoint Blockade. Cell. 2018; 175:984–997.e24. https://doi.org/10.1016/j.cell.2018.09.006 PMID:30388455

25. Eisenstein M. Making cancer immunotherapy a surer bet. Nature. 2017; 552:S72–73. https://doi.org/10.1038/d41586-017-08704-5 PMID:29293218

26. Reck M, Rodríguez-Abreu D, Robinson AG, Hui R, Csőszi T, Fülöp A, Gottfried M, Peled N, Tafreshi A, Cuffe S, O'Brien M, Rao S, Hotta K, et al, and KEYNOTE-024 Investigators. Pembrolizumab versus Chemotherapy for PD-L1-Positive Non-Small-Cell Lung Cancer. N Engl J Med. 2016; 375:1823–33. https://doi.org/10.1056/NEJMoa1606774 PMID:27718847

27. Ding W, LaPlant BR, Call TG, Parikh SA, Leis JF, He R, Shanafelt TD, Sinha S, Le-Rademacher J, Feldman AL, Habermann TM, Witzig TE, Wiseman GA, et al. Pembrolizumab in patients with CLL and Richter transformation or with relapsed CLL. Blood. 2017; 129:3419–27. https://doi.org/10.1182/blood-2017-02-765685 PMID:28424162

28. Balar AV, Castellano D, O'Donnell PH, Grivas P, Vuky J, Powles T, Plimack ER, Hahn NM, de Wit R, Pang L, Savage MJ, Perini RF, Keefe SM, et al. First-line pembrolizumab in cisplatin-ineligible patients with locally advanced and unresectable or metastatic urothelial cancer (KEYNOTE-052): a multicentre, single-arm, phase 2 study. Lancet Oncol. 2017; 18:1483–92. https://doi.org/10.1016/S1470-2045(17)30616-2 PMID:28967485

29. Sharma P, Callahan MK, Bono P, Kim J, Spiliopoulou P, Calvo E, Pillai RN, Ott PA, de Braud F, Morse M, Le DT, Jaeger D, Chan E, et al. Nivolumab monotherapy in recurrent metastatic urothelial carcinoma (CheckMate 032): a multicentre, open-label, two-stage, multi-arm, phase 1/2 trial. Lancet Oncol. 2016; 17:1590–98. https://doi.org/10.1016/S1470-2045(16)30496-X PMID:27733243

30. Yi M, Jiao D, Xu H, Liu Q, Zhao W, Han X, Wu K. Biomarkers for predicting efficacy of PD-1/PD-L1 inhibitors. Mol Cancer. 2018; 17:129. https://doi.org/10.1186/s12943-018-0864-3 PMID:30139382

31. Rizvi NA, Hellmann MD, Snyder A, Kvistborg P, Makarov V, Havel JJ, Lee W, Yuan J, Wong P, Ho TS, Miller ML, Rekhtman N, Moreira AL, et al. Cancer immunology. Mutational landscape determines sensitivity to PD-1 blockade in non-small cell lung cancer. Science. 2015; 348:124–28. https://doi.org/10.1126/science.aaa1348 PMID:25765070

32. Carbone DP, Reck M, Paz-Ares L, Creelan B, Horn L, Steins M, Felip E, van den Heuvel MM, Ciuleanu TE, Badin F, Ready N, Hiltermann TJ, Nair S, et al, and CheckMate 026 Investigators. First-Line Nivolumab in Stage IV or Recurrent Non-Small-Cell Lung Cancer. N Engl J Med. 2017; 376:2415–26. https://doi.org/10.1056/NEJMoa1613493 PMID:28636851

33. Hellmann MD, Ciuleanu TE, Pluzanski A, Lee JS, Otterson GA, Audigier-Valette C, Minenza E, Linardou H, Burgers S, Salman P, Borghaei H, Ramalingam SS, Brahmer J, et al. Nivolumab plus Ipilimumab in Lung Cancer with a High Tumor Mutational Burden. N Engl J Med. 2018; 378:2093–104. https://doi.org/10.1056/NEJMoa1801946 PMID:29658845

34. Seo JS, Kim A, Shin JY, Kim YT. Comprehensive analysis of the tumor immune micro-environment in non-small cell lung cancer for efficacy of checkpoint inhibitor. Sci Rep. 2018; 8:14576. https://doi.org/10.1038/s41598-018-32855-8 PMID:30275546

35. Song Q, Shang J, Yang Z, Zhang L, Zhang C, Chen J, Wu X. Identification of an immune signature predicting prognosis risk of patients in lung adenocarcinoma. J Transl Med. 2019; 17:70. https://doi.org/10.1186/s12967-019-1824-4 PMID:30832680

36. Goel S, DeCristo MJ, Watt AC, BrinJones H, Sceneay J, Li BB, Khan N, Ubellacker JM, Xie S, Metzger-Filho O, Hoog J, Ellis MJ, Ma CX, et al. CDK4/6 inhibition triggers anti-tumour immunity. Nature. 2017; 548:471–75. https://doi.org/10.1038/nature23465 PMID:28813415

37. Smith CC, Beckermann KE, Bortone DS, De Cubas AA, Bixby LM, Lee SJ, Panda A, Ganesan S, Bhanot G, Wallen EM, Milowsky MI, Kim WY, Rathmell WK, et al. Endogenous retroviral signatures predict immunotherapy response in clear cell renal cell carcinoma. J Clin Invest. 2018; 128:4804–20. https://doi.org/10.1172/JCI121476 PMID:30137025

38. Li VD, Li KH, Li JT. TP53 mutations as potential prognostic markers for specific cancers: analysis of data from The Cancer Genome Atlas and the International Agency for Research on Cancer TP53 Database. J Cancer Res Clin Oncol. 2019; 145:625–36. https://doi.org/10.1007/s00432-018-2817-z PMID:30542790

39. Aisner DL, Sholl LM, Berry LD, Rossi MR, Chen H, Fujimoto J, Moreira AL, Ramalingam SS, Villaruz LC, Otterson GA, Haura E, Politi K, Glisson B, et al, and LCMC2 investigators. The Impact of Smoking and TP53 Mutations in Lung Adenocarcinoma Patients with Targetable Mutations-The Lung Cancer Mutation Consortium (LCMC2). Clin Cancer Res. 2018; 24: 1038–47. https://doi.org/10.1158/1078-0432.CCR-17-2289 PMID:29217530

40. Dong ZY, Zhong WZ, Zhang XC, Su J, Xie Z, Liu SY, Tu HY, Chen HJ, Sun YL, Zhou Q, Yang JJ, Yang XN, Lin JX, et al. Potential Predictive Value of *TP53* and *KRAS* Mutation Status for Response to PD-1 Blockade Immunotherapy in Lung Adenocarcinoma. Clin Cancer Res. 2017; 23:3012–24. https://doi.org/10.1158/1078-0432.CCR-16-2554 PMID:28039262

41. Brahmer JR, Tykodi SS, Chow LQ, Hwu WJ, Topalian SL, Hwu P, Drake CG, Camacho LH, Kauh J, Odunsi K, Pitot HC, Hamid O, Bhatia S, et al. Safety and activity of anti-PD-L1 antibody in patients with advanced cancer. N Engl J Med. 2012; 366:2455–65. https://doi.org/10.1056/NEJMoa1200694 PMID:22658128

42. Alexandrov LB, Nik-Zainal S, Wedge DC, Aparicio SA, Behjati S, Biankin AV, Bignell GR, Bolli N, Borg A, Børresen-Dale AL, Boyault S, Burkhardt B, Butler AP, et al, and Australian Pancreatic Cancer Genome Initiative, and ICGC Breast Cancer Consortium, and ICGC MMML-Seq Consortium, and ICGC PedBrain. Signatures of mutational processes in human cancer. Nature. 2013; 500:415–21. https://doi.org/10.1038/nature12477 PMID:23945592

43. Thorsson V, Gibbs DL, Brown SD, Wolf D, Bortone DS, Ou Yang TH, Porta-Pardo E, Gao GF, Plaisier CL, Eddy JA, Ziv E, Culhane AC, Paull EO, et al. The Immune Landscape of Cancer. Immunity. 2018; 48:812–830.e14. https://doi.org/10.1016/j.immuni.2018.03.023 PMID:29628290

44. Wolf DM, Lenburg ME, Yau C, Boudreau A, van 't Veer LJ. Gene co-expression modules as clinically relevant hallmarks of breast cancer diversity. PLoS One. 2014; 9:e88309. https://doi.org/10.1371/journal.pone.0088309 PMID:24516633

45. Cheng WY, Ou Yang TH, Anastassiou D. Biomolecular events in cancer revealed by attractor metagenes. PLoS Comput Biol. 2013; 9:e1002920. https://doi.org/10.1371/journal.pcbi.1002920 PMID:23468608

46. Cheng WY, Ou Yang TH, Anastassiou D. Development of a prognostic model for breast cancer survival in an open challenge environment. Sci Transl Med. 2013; 5:181ra50. https://doi.org/10.1126/scitranslmed.3005974 PMID:23596202

47. Bedognetti D, Hendrickx W, Ceccarelli M, Miller LD, Seliger B. Disentangling the relationship between tumor genetic programs and immune responsiveness. Curr Opin Immunol. 2016; 39:150–58. https://doi.org/10.1016/j.coi.2016.02.001 PMID:26967649

48. Galon J, Angell HK, Bedognetti D, Marincola FM. The continuum of cancer immunosurveillance: prognostic, predictive, and mechanistic signatures. Immunity. 2013; 39:11–26. https://doi.org/10.1016/j.immuni.2013.07.008 PMID:23890060

49. Hendrickx W, Simeone I, Anjum S, Mokrab Y, Bertucci F, Finetti P, Curigliano G, Seliger B, Cerulo L, Tomei S, Delogu LG, Maccalli C, Wang E, et al. Identification of genetic determinants of breast cancer immune phenotypes by integrative genome-scale analysis. Oncoimmunology. 2017; 6:e1253654. https://doi.org/10.1080/2162402X.2016.1253654 PMID:28344865

50. Şenbabaoğlu Y, Gejman RS, Winer AG, Liu M, Van Allen EM, de Velasco G, Miao D, Ostrovnaya I, Drill E, Luna A, Weinhold N, Lee W, Manley BJ, et al. Tumor immune microenvironment characterization in clear

cell renal cell carcinoma identifies prognostic and immunotherapeutically relevant messenger RNA signatures. Genome Biol. 2016; 17:231. https://doi.org/10.1186/s13059-016-1092-z PMID:27855702

51. Gentles AJ, Newman AM, Liu CL, Bratman SV, Feng W, Kim D, Nair VS, Xu Y, Khuong A, Hoang CD, Diehn M, West RB, Plevritis SK, Alizadeh AA. The prognostic landscape of genes and infiltrating immune cells across human cancers. Nat Med. 2015; 21:938–45. https://doi.org/10.1038/nm.3909 PMID:26193342

52. Bindea G, Mlecnik B, Tosolini M, Kirilovsky A, Waldner M, Obenauf AC, Angell H, Fredriksen T, Lafontaine L, Berger A, Bruneval P, Fridman WH, Becker C, et al. Spatiotemporal dynamics of intratumoral immune cells reveal the immune landscape in human cancer. Immunity. 2013; 39:782–95. https://doi.org/10.1016/j.immuni.2013.10.003 PMID:24138885

53. Godec J, Tan Y, Liberzon A, Tamayo P, Bhattacharya S, Butte AJ, Mesirov JP, Haining WN. Compendium of Immune Signatures Identifies Conserved and Species-Specific Biology in Response to Inflammation. Immunity. 2016; 44:194–206. https://doi.org/10.1016/j.immuni.2015.12.006 PMID:26795250

54. Subramanian A, Tamayo P, Mootha VK, Mukherjee S, Ebert BL, Gillette MA, Paulovich A, Pomeroy SL, Golub TR, Lander ES, Mesirov JP. Gene set enrichment analysis: a knowledge-based approach for interpreting genome-wide expression profiles. Proc Natl Acad Sci USA. 2005; 102:15545–50. https://doi.org/10.1073/pnas.0506580102 PMID:16199517

55. Brunet JP, Tamayo P, Golub TR, Mesirov JP. Metagenes and molecular pattern discovery using matrix factorization. Proc Natl Acad Sci USA. 2004; 101:4164–69. https://doi.org/10.1073/pnas.0308531101 PMID:15016911

56. Gao Y, Church G. Improving molecular cancer class discovery through sparse non-negative matrix factorization. Bioinformatics. 2005; 21:3970–75. https://doi.org/10.1093/bioinformatics/bti653 PMID:16244221

57. Kim H, Park H. Sparse non-negative matrix factorizations via alternating non-negativity-constrained least squares for microarray data analysis. Bioinformatics. 2007; 23:1495–502. https://doi.org/10.1093/bioinformatics/btm134 PMID:17483501

58. Gaujoux R, Seoighe C. A flexible R package for nonnegative matrix factorization. BMC Bioinformatics. 2010; 11:367. https://doi.org/10.1186/1471-2105-11-367 PMID:20598126

59. Kim J, Mouw KW, Polak P, Braunstein LZ, Kamburov A, Kwiatkowski DJ, Rosenberg JE, Van Allen EM, D'Andrea A, Getz G. Somatic ERCC2 mutations are associated with a distinct genomic signature in urothelial tumors. Nat Genet. 2016; 48:600–06. https://doi.org/10.1038/ng.3557 PMID:27111033

60. Ritchie ME, Phipson B, Wu D, Hu Y, Law CW, Shi W, Smyth GK. limma powers differential expression analyses for RNA-sequencing and microarray studies. Nucleic Acids Res. 2015; 43:e47. https://doi.org/10.1093/nar/gkv007 PMID:25605792

61. Love MI, Huber W, Anders S. Moderated estimation of fold change and dispersion for RNA-seq data with DESeq2. Genome Biol. 2014; 15:550. https://doi.org/10.1186/s13059-014-0550-8 PMID:25516281

62. Liberzon A, Subramanian A, Pinchback R, Thorvaldsdóttir H, Tamayo P, Mesirov JP. Molecular signatures database (MSigDB) 3.0. Bioinformatics. 2011; 27:1739–40. https://doi.org/10.1093/bioinformatics/btr260 PMID:21546393

63. Lawrence MS, Stojanov P, Polak P, Kryukov GV, Cibulskis K, Sivachenko A, Carter SL, Stewart C, Mermel CH, Roberts SA, Kiezun A, Hammerman PS, McKenna A, et al. Mutational heterogeneity in cancer and the search for new cancer-associated genes. Nature. 2013; 499:214–18. https://doi.org/10.1038/nature12213 PMID:23770567

64. Kandoth C, McLellan MD, Vandin F, Ye K, Niu B, Lu C, Xie M, Zhang Q, McMichael JF, Wyczalkowski MA, Leiserson MD, Miller CA, Welch JS, et al. Mutational landscape and significance across 12 major cancer types. Nature. 2013; 502:333–39. https://doi.org/10.1038/nature12634 PMID:24132290

65. Klijn C, Durinck S, Stawiski EW, Haverty PM, Jiang Z, Liu H, Degenhardt J, Mayba O, Gnad F, Liu J, Pau G, Reeder J, Cao Y, et al. A comprehensive transcriptional portrait of human cancer cell lines. Nat Biotechnol. 2015; 33:306–12. https://doi.org/10.1038/nbt.3080 PMID:25485619

SUPPLEMENTARY MATERIALS

2995 immune-related genes

We obtained these 2995 immune-related genes from 160 immune signatures curated in a previous study [1], which was based on 11 immune relevant studies. Eighty-three of these 160 immune signatures were cancer immune response-related signatures, whereas the remaining 77 signatures are of general validity for immunity. These 83 signatures consisted of 68 gene sets from a earlier study [2], 9 signatures derived from TCGA gene expression data (immune metagene attractors) [3, 4], 3 signatures representing immune contexture function [5–7], and 3 signatures from a recent study [8]. The remaining 77 signatures comprised of 45 immune-cell specific signatures from 2 sources [9, 10], and 32 signatures from the ImmuneSigDB [11, 12].

Main *R* codes used in this study

```
# Nonnegative matrix factorization (NMF)
        library(NMF)
        estim.r <- nmf(gene_expression_matrix, 2:6,
        nrun = 200, method = 'brunet')
        plot(estim.r)
        consensusmap(estim.r)
        fit <- nmf(gene_expression_matrix, 2, nrun =
        200, method = "brunet")
        subtype.result <- predict(fit)
# Gene set enrichment analysis (GSEA)
        library(fgsea)
library(ggplot2)
        fgsea.result <- fgsea(pathways =
        annotation_pathways,
            stats = genes_rank_list,
            minSize = 15,
            maxSize = 500,
            nperm = 1000000)
        plotEnrichment(path[["pathway_name"]],
        genes_rank_list)
# Waterfall plot
        library(GenVisR)
waterfall(mutation_data, plotGenes = genes_to_plot,
        mainDropMut = TRUE, coverageSpace =
        30000000, clinDat = clinical_data)
# Multivariate regression model
        library(forestmodel)
library(survival)
forest_model(coxph(Surv(survival_time, survival_end)
~ variables, related_data), factor_separate_line = T)
forest_model(glm(categorical variable ~ variables,
binomial(), related_data), factor_separate_line = T))
```

REFERENCES

1. Thorsson V, Gibbs DL, Brown SD, Wolf D, Bortone DS, Ou Yang TH, Porta-Pardo E, Gao GF, Plaisier CL, Eddy JA, Ziv E, Culhane AC, Paull EO, et al. The Immune Landscape of Cancer. Immunity. 2018; 48:812–830.e14. https://doi.org/10.1016/j.immuni.2018.03.023 PMID:29628290

2. Wolf DM, Lenburg ME, Yau C, Boudreau A, van 't Veer LJ. Gene co-expression modules as clinically relevant hallmarks of breast cancer diversity. PLoS One. 2014; 9:e88309. https://doi.org/10.1371/journal.pone.0088309 PMID:24516633

3. Cheng WY, Ou Yang TH, Anastassiou D. Biomolecular events in cancer revealed by attractor metagenes. PLOS Comput Biol. 2013; 9:e1002920. https://doi.org/10.1371/journal.pcbi.1002920 PMID:23468608

4. Cheng WY, Ou Yang TH, Anastassiou D. Development of a prognostic model for breast cancer survival in an open challenge environment. Sci Transl Med. 2013; 5:181ra50. https://doi.org/10.1126/scitranslmed.3005974 PMID:23596202

5. Bedognetti D, Hendrickx W, Ceccarelli M, Miller LD, Seliger B. Disentangling the relationship between tumor genetic programs and immune responsiveness. Curr Opin Immunol. 2016; 39:150–58. https://doi.org/10.1016/j.coi.2016.02.001 PMID:26967649

6. Galon J, Angell HK, Bedognetti D, Marincola FM. The continuum of cancer immunosurveillance: prognostic, predictive, and mechanistic signatures. Immunity. 2013; 39:11–26. https://doi.org/10.1016/j.immuni.2013.07.008 PMID:23890060

7. Hendrickx W, Simeone I, Anjum S, Mokrab Y, Bertucci F, Finetti P, Curigliano G, Seliger B, Cerulo L, Tomei S, Delogu LG, Maccalli C, Wang E, et al. Identification of genetic determinants of breast cancer immune phenotypes by integrative genome-scale analysis. OncoImmunology. 2017; 6:e1253654. https://doi.org/10.1080/2162402X.2016.1253654 PMID:28344865

8. Şenbabaoğlu Y, Gejman RS, Winer AG, Liu M, Van Allen EM, de Velasco G, Miao D, Ostrovnaya I, Drill E, Luna A, Weinhold N, Lee W, Manley BJ, et al. Tumor immune microenvironment characterization in clear

cell renal cell carcinoma identifies prognostic and immunotherapeutically relevant messenger RNA signatures. Genome Biol. 2016; 17:231. https://doi.org/10.1186/s13059-016-1092-z PMID:27855702

9. Gentles AJ, Newman AM, Liu CL, Bratman SV, Feng W, Kim D, Nair VS, Xu Y, Khuong A, Hoang CD, Diehn M, West RB, Plevritis SK, Alizadeh AA. The prognostic landscape of genes and infiltrating immune cells across human cancers. Nat Med. 2015; 21:938–45. https://doi.org/10.1038/nm.3909 PMID:26193342

10. Bindea G, Mlecnik B, Tosolini M, Kirilovsky A, Waldner M, Obenauf AC, Angell H, Fredriksen T, Lafontaine L, Berger A, Bruneval P, Fridman WH, Becker C, et al. Spatiotemporal dynamics of intratumoral immune cells reveal the immune landscape in human cancer. Immunity. 2013; 39:782–95. https://doi.org/10.1016/j.immuni.2013.10.003 PMID:24138885

11. Godec J, Tan Y, Liberzon A, Tamayo P, Bhattacharya S, Butte AJ, Mesirov JP, Haining WN. Compendium of Immune Signatures Identifies Conserved and Species-Specific Biology in Response to Inflammation. Immunity. 2016; 44:194–206. https://doi.org/10.1016/j.immuni.2015.12.006 PMID:26795250

12. Subramanian A, Tamayo P, Mootha VK, Mukherjee S, Ebert BL, Gillette MA, Paulovich A, Pomeroy SL, Golub TR, Lander ES, Mesirov JP. Gene set enrichment analysis: a knowledge-based approach for interpreting genome-wide expression profiles. Proc Natl Acad Sci USA. 2005; 102:15545–50. https://doi.org/10.1073/pnas.0506580102 PMID:16199517

Supplementary Figures

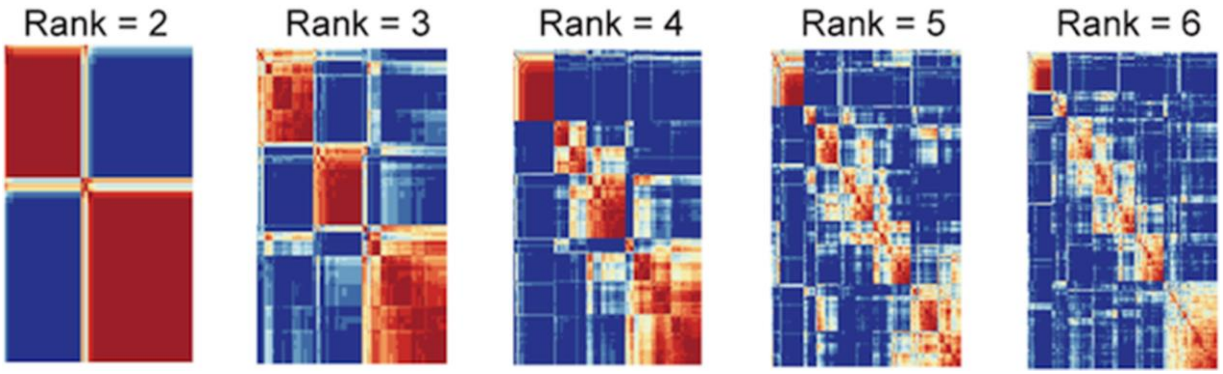

Supplementary Figure 1. Heatmap representation of NMF clustering.

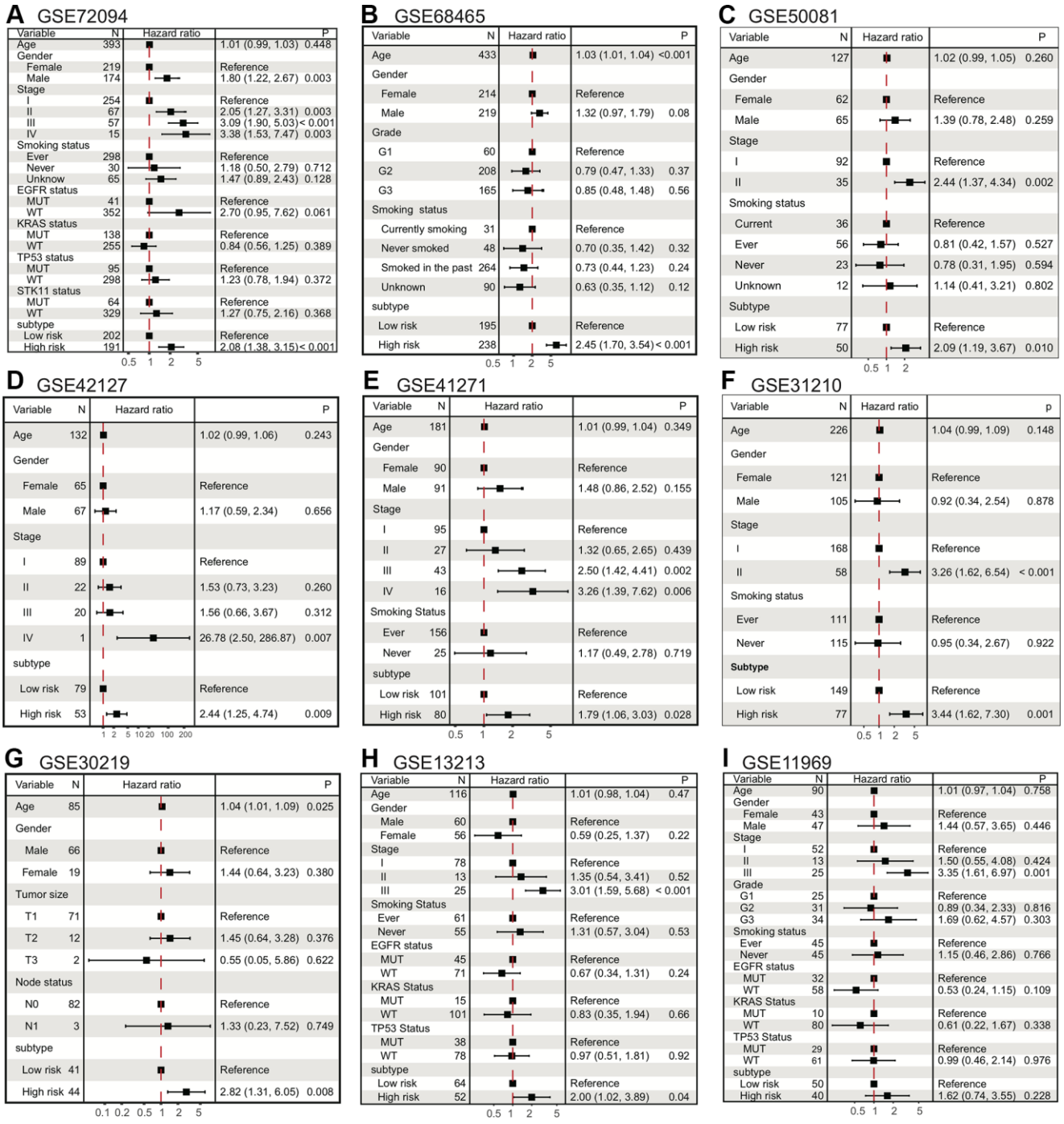

Supplementary Figure 2. Prognostic significance of high-risk versus low-risk subtypes using multivariate Cox model in 9 validation cohorts of (**A**) GSE72094, (**B**) GSE68465, (**C**) GSE50081, (**D**) GSE42127, (**E**) GSE41271, (**F**) GSE31210, (**G**) GSE30219, (**H**) GSE13213, and (**I**) GSE11969.

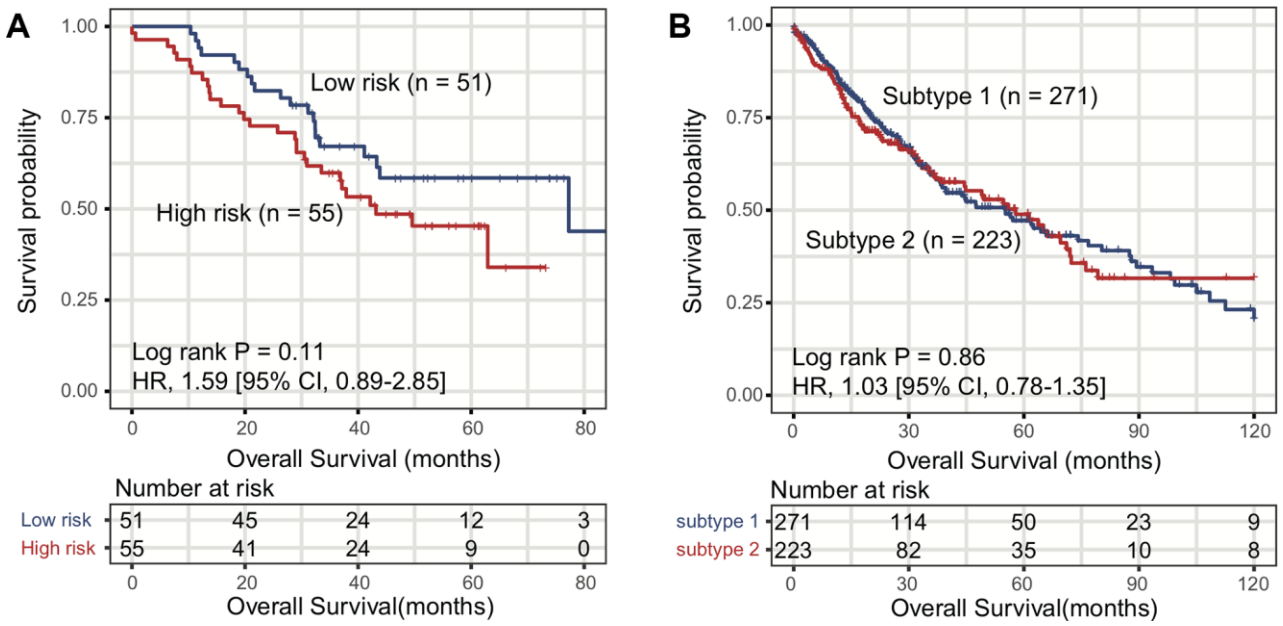

Supplementary Figure 3. (**A**) Kaplan-Meier plot of identified 2 subtypes in GSE81089 dataset. (**B**) Kaplan-Meier plot of identified TCGA LUSC subtypes.

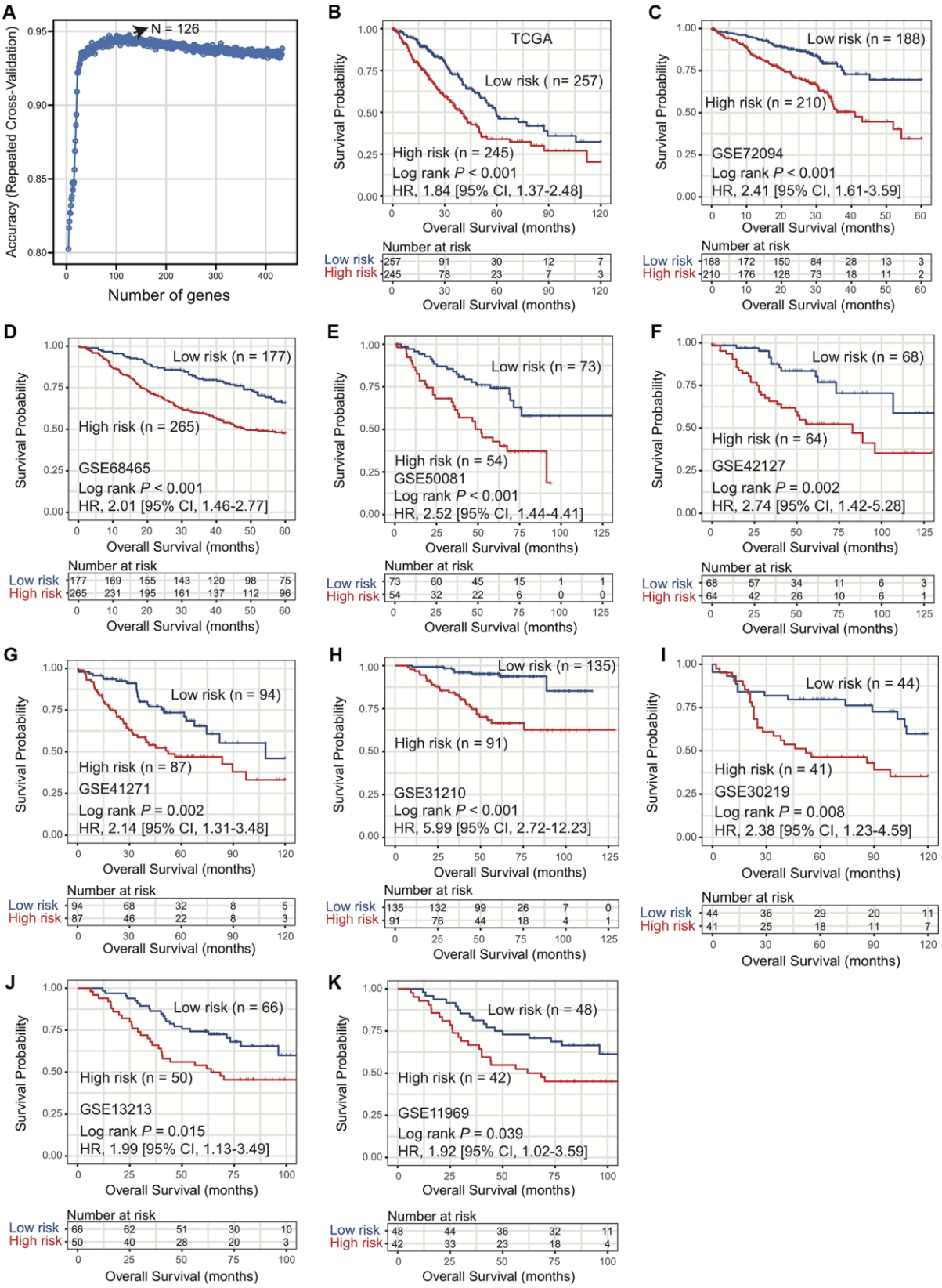

Supplementary Figure 4. (**A**) Relation between classification accuracy and selected genes via recursive feature elimination algorithm. (**B**–**K**) Keplan-Meier plot of identified subtypes using 126 genes in TCGA and 9 validation cohorts.

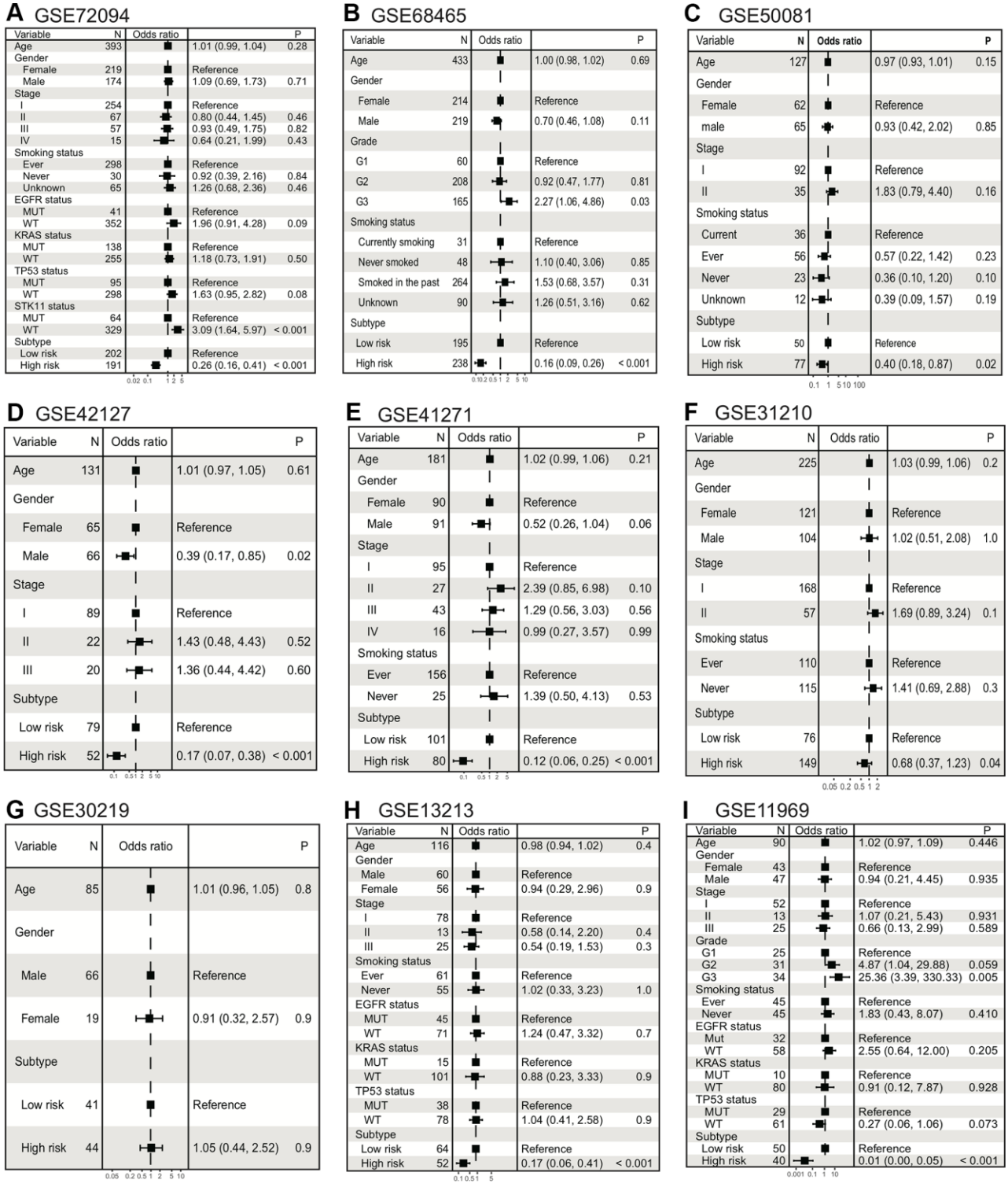

Supplementary Figure 5. Association of identified LUAD subtypes with TIDE socre using multivariate logistic analysis in 9 validation cohorts of (**A**) GSE72094, (**B**) GSE68465, (**C**) GSE50081, (**D**) GSE42127, (**E**) GSE41271, (**F**) GSE31210, (**G**) GSE30219, (**H**) GSE13213, and (**I**) GSE11969.

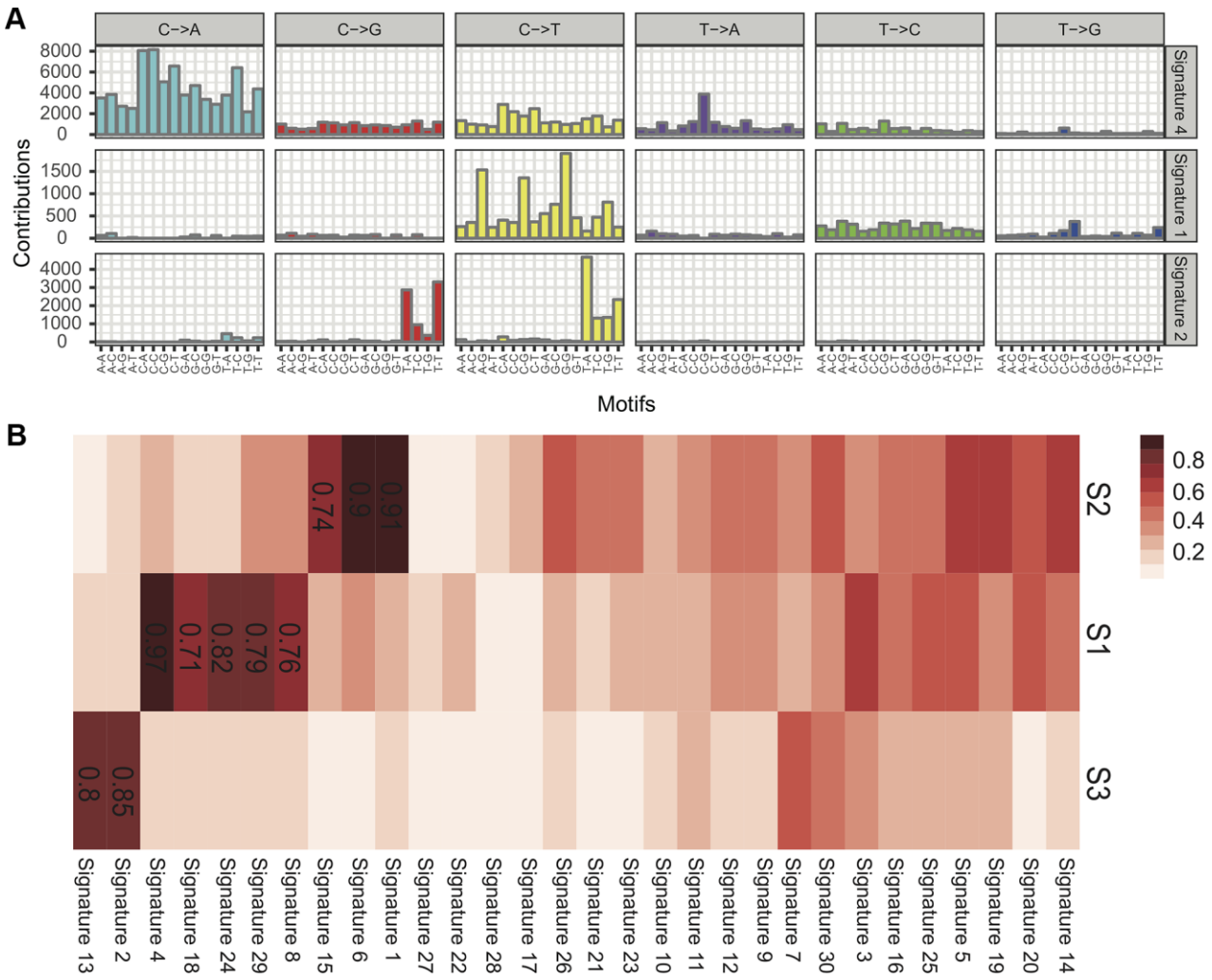

Supplementary Figure 6. (**A**) Mutational signatures extracted from TCGA LUAD cohort and (**B**) their cosine similarity with COSMIC mutational signatures.

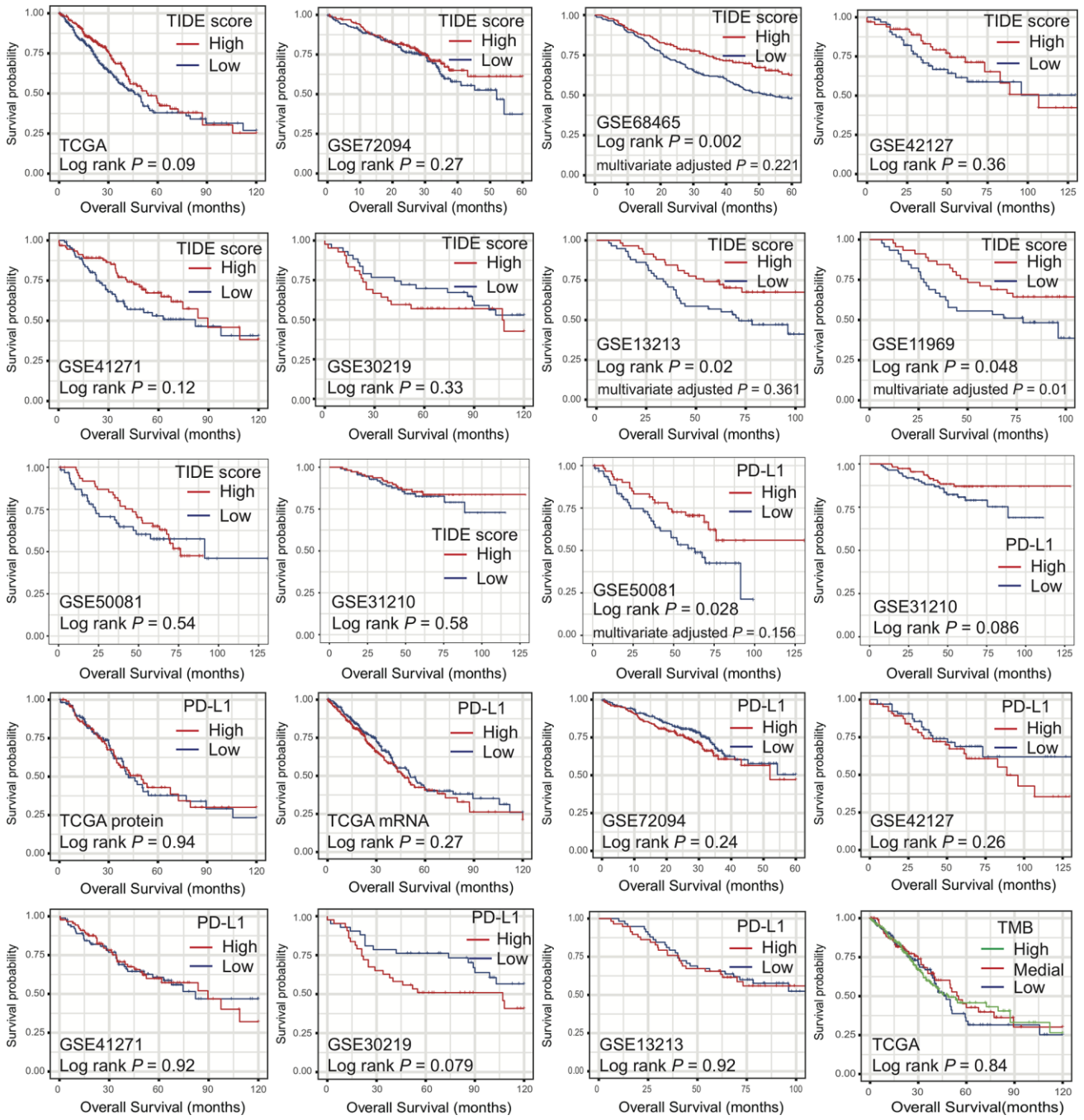

Supplementary Figure 7. Kaplan-Meier plots with respect to TIDE score, *PD-L1* expression, and TMB in TCGA and 9 validation cohorts.

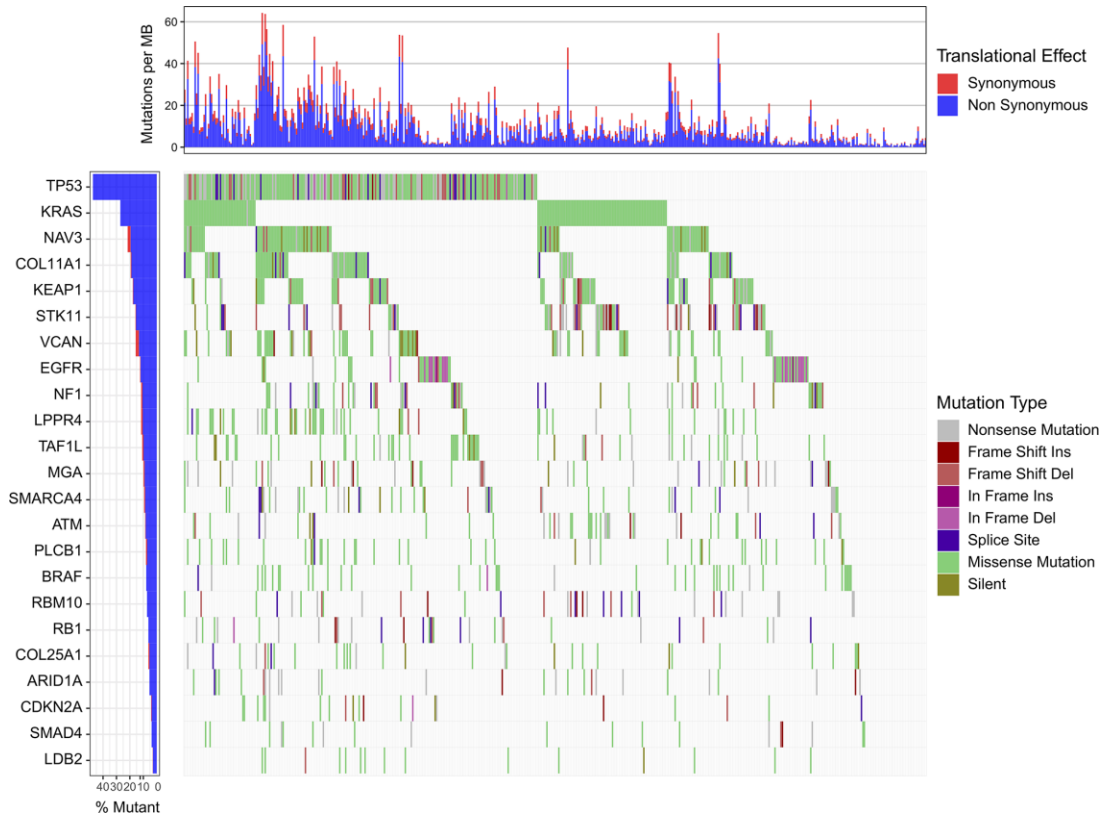

Supplementary Figure 8. Mutational landscape of SMGs in TCGA LUAD cohort.

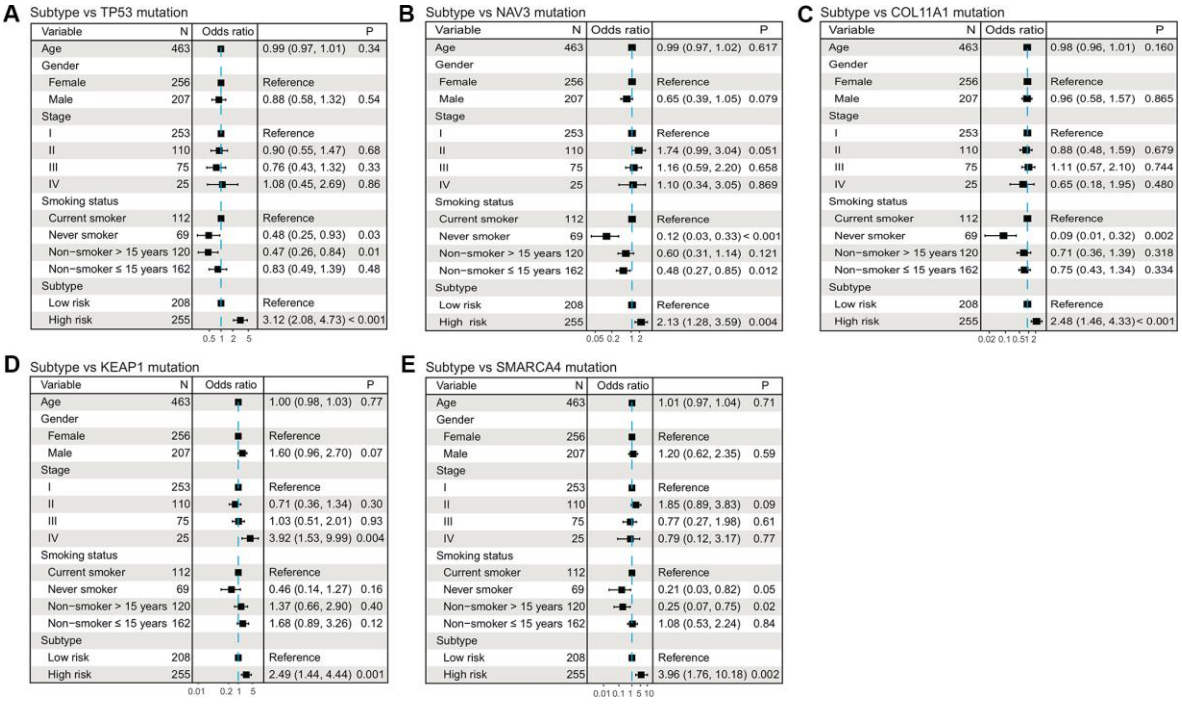

Supplementary Figure 9. Associations between mutations in *TP53*, *NAV3*, *CLO11A1*, *KEAP1* and *SMARCA4* and identified 2 LUAD subtypes using multivariate logistic analysis.

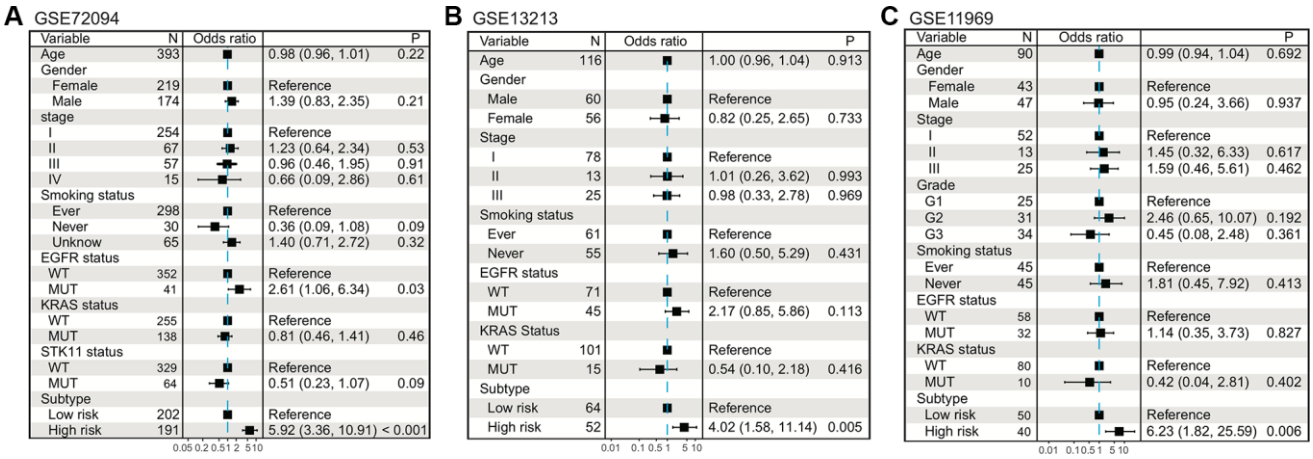

Supplementary Figure 10. Associations of *TP53* mutation with high-risk subtype in (**A**) GSE72094, (**B**) GSE13213 and (**C**) GSE11969.

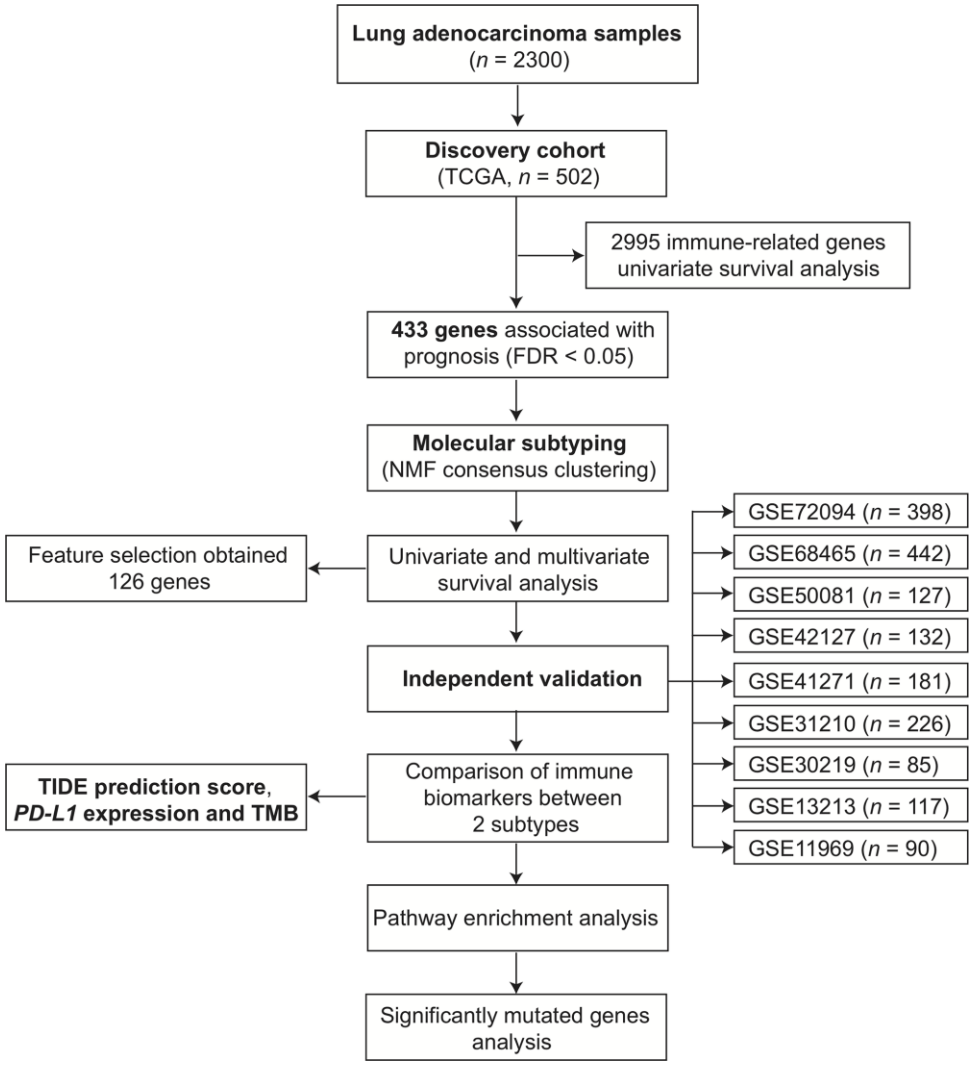

Supplementary Figure 11. Flow chart of our study. TCGA and 9 public LUAD cohorts containing 2300 samples were included to peroform relevant analyses.

Supplementary Tables

Please browse Full Text version to see the data of Supplementary Table 1

Supplementary Table 1. 433 genes with FDR less than 0.05 in univariate survival analysis.

Supplementary Table 2. 126 genes were obtained through RFE features selection.

Gene	Entrezid	Gene	Entrezid	Gene	Entrezid	Gene	Entrezid
TSPAN32	10077	NCR3	259197	MCM10	55388	CCNB1	891
RASGRP2	10235	ASPM	259266	DEPDC1	55635	SELENBP1	8991
CDKN3	1033	STAP1	26228	PBK	55872	PRC1	9055
NDC80	10403	AMPD1	270	KIF15	56992	CD1B	910
CENPA	1058	HPGDS	27306	PTGDS	5730	CD1C	911
CENPE	1062	GNG7	2788	SPC25	57405	CD1D	912
RAD51AP1	10635	LINC00926	283663	DNASE2B	58511	CD1E	913
PLK4	10733	C11orf21	29125	RGS13	6003	CCNB2	9133
KIF2C	11004	RACGAP1	29127	RRM2	6241	EXO1	9156
UBE2C	11065	HLA-DOB	3112	BLK	640	CD5	921
CHEK1	1111	BIRC3	330	NCAPG	64151	AURKB	9212
ZWINT	11130	BIRC5	332	SFTPB	6439	CACNA2D2	9254
OIP5	11339	IL16	3603	SLAMF1	6504	CD19	930
FCRL1	115350	KLRB1	3820	SLC18A2	6571	MS4A1	931
CCR6	1235	KIF11	3832	SPIB	6689	SIGLEC6	946
ADH1A	124	LY9	4063	AURKA	6790	KIF23	9493
ADH1B	125	MAD2L1	4085	BUB1B	701	CD40LG	959
COL4A3	1285	MAL	4118	TK1	7083	ESPL1	9700
CR2	1380	MKI67	4288	CLEC3B	7123	CD79A	973
CTSG	1511	MYBL2	4605	TOP2A	7153	CD79B	974
DNASE1L3	1776	NEK2	4751	TTK	7272	ACAP1	9744
FAM129C	199786	PAX5	5079	CCR2	729230	DLGAP5	9787
SKA1	220134	NUSAP1	51203	VIPR1	7433	CDK1	983
MS4A2	2206	GTSE1	51512	DSCC1	79075	MELK	9833
FCER2	2208	PLK1	5347	ANKRD55	79722	CDC6	990
TMEM130	222865	POLE2	5427	CXorf21	80231	CDC20	991
TPX2	22974	ERCC6L	54821	TRAF3IP3	80342	KIF14	9928
FOXM1	2305	PARPBP	55010	TLR10	81793	CD302	9936
NCAPH	23397	CEP55	55165	CDC45	8318	CDC25C	995
TNFRSF13B	23495	FANCI	55215	ATP13A4	84239	HS3ST2	9956
LILRA4	23547	NEIL3	55247	FCRLA	84824		
KIF4A	24137	HJURP	55355	CCNA2	890		

Supplementary Table 3. Distinct clinical characteristics between 2 LUAD subtypes.

Characteristics	Low risk (*n*=210)	High risk (*n*=256)	*P*
Age (years)	66.6±9.1	64.2±10.6	0.125
Gender			
Female	137 (65.2)	120 (46.9)	
Male	73 (34.8)	136 (53.1)	
Stage			
I	139 (66.2)	115 (44.9)	
II	38 (18.1)	74 (28.9)	
III	25 (11.9)	50 (19.5)	
IV	8 (3.8)	17 (6.6)	
Smoking status			
Never smoker	39 (18.6)	31 (12.1)	
Non-smoker>15 years	69 (32.9)	52 (20.3)	
Non-smoker≤15 years	67 (31.9)	95 (37.1)	
Current smoker	35 (16.7)	78 (30.5)	

Supplementary Table 4. Summary of TCGA and 9 validation datasets included in this study.

Datasets	Platforms	Sample size
TCGA	Illumina RNAseq HTSeq	502
GSE72094	Rosetta/Merck Human RSTA Custom Affymetrix 2.0 microarray	398
GSE68465	Affymetrix Human Genome U133A Array	442
GSE50081	Affymetrix Human Genome U133 Plus 2.0 Array	127
GSE42127	Illumina HumanWG-6 v3.0 expression beadchip	132
GSE41271	Illumina HumanWG-6 v3.0 expression beadchip	181
GSE31210	Affymetrix Human Genome U133 Plus 2.0 Array	226
GSE30219	Affymetrix Human Genome U133 Plus 2.0 Array	85
GSE13213	Agilent-014850 Whole Human Genome Microarray 4x44K G4112F	117
GSE11969	Agilent Homo sapiens 21.6K custom array	90
Total		2300

Supplementary Table 5. Descriptions of clinical characteristics for LUAD patients in TCGA and 9 validation datasets.

Characteristics	TCGA	GSE72094	GSE68465	GSE50081	GSE42127	GSE41271	GSE31210	GSE30219	GSE13213	GSE11969
Number of	502	398	422	127	132	181	226	85	117	90
Age (years)	65.3 ± 9.9	69.4 ± 9.5	64.5 ± 10.1	68.7 ± 9.7	65.8 ± 10.3	64.6 ± 10.4	59.6 ± 7.4	61.5 ± 9.3	60.7 ± 10.2	61.1 ± 9.8
Gender										
Male	209	174	219	65	67	91	105	66	60	47
Female	257	219	214	62	65	90	121	19	56	43
Stage	254	254		92	89	95	168		78	52
II	112	67	-	35	22	27	58	-	13	13
III	75	57	-	0	20	43	0	-	25	25
IV	25	15	-	0	1	16	0	-	-	-
Grade										
G1			60							25
G2	-	-	208	-	-	-	-	-	-	31
G3	-	-	165	-	-	-	-	-	-	34
Smoking status Never smoker	70	298	15	23		25	111		55	45
Ever smoker	-	30	94	56	-	156	115	-	61	45
Current smoker	113	-	16	36	-	-	-	-	-	-
Non-smoker>15	121	-	-	-	-	-	-	-	-	-
Non-smoker≤ 15 years	162	-	-	-	-	-	-	-	-	-
NA	-	65	90	12	-	-	-	-	-	-